Recombinant BCG Expressing ESX-1 of Mycobacterium marinum Combines Low Virulence with Cytosolic Immune Signaling and Improved TB Protection.

Matthias I Gröschel, Fadel Sayes, Sung Jae Shin, Wafa Frigui, Alexandre Pawlik, Mickael Orgeur, Robin Canetti, Nadine Honoré, Roxane Simeone, Tjip S van Der Werf, et al.

Article

Cell Reports

Recombinant BCG Expressing ESX-1 of *Mycobacterium marinum* Combines Low Virulence with Cytosolic Immune Signaling and Improved TB Protection

Graphical Abstract

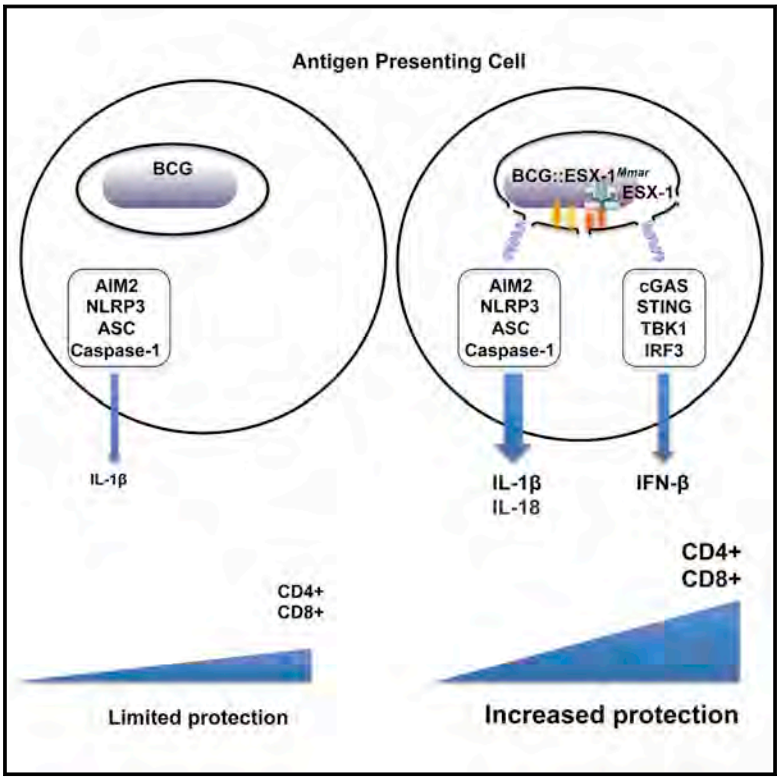

Highlights

- BCG expressing the ESX-1 T7 secretion system of *M. marinum* induces phagosomal rupture
- Rupture-induced innate immune signaling leads to IFN-β and enhanced IL-1β release
- ESX-1 signaling induces $CD8^+$ and Ag-specific $CD4^+$ T cell responses and high protection
- Recombinant BCG-expressing ESX-1 of BSL2 organism *M. marinum* shows low virulence

Authors

Matthias I. Gröschel, Fadel Sayes, Sung Jae Shin, ..., Sang-Nae Cho, Laleh Majlessi, Roland Brosch

Correspondence

roland.brosch@pasteur.fr

In Brief

Gröschel et al. describe the virulence-neutral expression of the ESX-1 type VII secretion system of *Mycobacterium marinum* in the attenuated BCG vaccine. ESX-1-marinum enables recombinant BCG to rupture the phagosome and to induce cytosolic pattern recognition and dedicated innate immune signaling in mice, resulting in increased protection against tuberculosis.

Gröschel et al., 2017, Cell Reports *18*, 2752–2765
March 14, 2017
http://dx.doi.org/10.1016/j.celrep.2017.02.057

OPEN ACCESS
CellPress

Cell Reports
Article

Recombinant BCG Expressing ESX-1 of *Mycobacterium marinum* Combines Low Virulence with Cytosolic Immune Signaling and Improved TB Protection

Matthias I. Gröschel,[1,2] Fadel Sayes,[1] Sung Jae Shin,[3] Wafa Frigui,[1] Alexandre Pawlik,[1] Mickael Orgeur,[1] Robin Canetti,[1] Nadine Honoré,[1] Roxane Simeone,[1] Tjip S. van der Werf,[2] Wilbert Bitter,[4,5] Sang-Nae Cho,[3] Laleh Majlessi,[1] and Roland Brosch[1,6,*]

[1]Unit for Integrated Mycobacterial Pathogenomics, Institut Pasteur, 75015 Paris, France
[2]Department of Pulmonary Diseases & Tuberculosis, University Medical Center Groningen, University of Groningen, 9700 RB Groningen, the Netherlands
[3]Department of Microbiology, Institute for Immunology and Immunological Diseases, Brain Korea 21 PLUS Project for Medical Science, Yonsei University College of Medicine, 03722 Seoul, South Korea
[4]Department of Medical Microbiology and Infection Control, VU University Medical Center, 1081 HZ Amsterdam, the Netherlands
[5]Section Molecular Microbiology, Amsterdam Institute of Molecules, Medicine and Systems, Vrije Universiteit Amsterdam, 1081 HZ Amsterdam, the Netherlands
[6]Lead Contact
*Correspondence: roland.brosch@pasteur.fr
http://dx.doi.org/10.1016/j.celrep.2017.02.057

SUMMARY

Recent insights into the mechanisms by which *Mycobacterium tuberculosis*, the etiologic agent of human tuberculosis, is recognized by cytosolic nucleotide sensors have opened new avenues for rational vaccine design. The only licensed anti-tuberculosis vaccine, *Mycobacterium bovis* BCG, provides limited protection. A feature of BCG is the partial deletion of the ESX-1 type VII secretion system, which governs phagosomal rupture and cytosolic pattern recognition, key intracellular phenotypes linked to increased immune signaling. Here, by heterologously expressing the *esx-1* region of *Mycobacterium marinum* in BCG, we engineered a low-virulence, ESX-1-proficient, recombinant BCG (BCG::ESX-1^{Mmar}) that induces the cGas/STING/TBK1/IRF-3/type I interferon axis and enhances AIM2 and NLRP3 inflammasome activity, resulting in both higher proportions of CD8$^+$ T cell effectors against mycobacterial antigens shared with BCG and polyfunctional CD4$^+$ Th1 cells specific to ESX-1 antigens. Importantly, independent mouse vaccination models show that BCG::ESX-1^{Mmar} confers superior protection relative to parental BCG against challenges with highly virulent *M. tuberculosis*.

INTRODUCTION

Tuberculosis (TB) is a chronic infectious disease caused by *Mycobacterium tuberculosis* that continues to be among the top five causes of death in 18 countries (GBD 2013 Mortality and Causes of Death Collaborators, 2015). Increased prevention would be a tremendous asset in controlling the global epidemic, as reflected by World Health Organization's new End TB Strategy (Uplekar et al., 2015). Rational design of an improved vaccine that is able to prevent active disease would be the most effective measure in TB control (Knight et al., 2014). Thus, numerous efforts are being undertaken to develop improved anti-TB vaccines, some of which have recently entered clinical development (Fletcher et al., 2016; Grode et al., 2013; Spertini et al., 2015).

The currently licensed anti-TB vaccine *Mycobacterium bovis* BCG, also known as Bacille Calmette Guérin, confers insufficient protection against pulmonary TB in adolescents and adults (Kaufmann et al., 2015). The absence of a 9.5-kb genomic region across all BCG strains, termed Region of Difference 1 (RD1), is the principal molecular determinant underlying BCG attenuation (Hsu et al., 2003; Pym et al., 2002). RD1 harbors genes required for the paradigm type VII secretion (T7S) ESX-1, or ESAT-6 secretion system that is dedicated to the export of proteins that play key roles in host-pathogen interactions and pathogenic potential (Gröschel et al., 2016). During infection of host phagocytes, a functional ESX-1 secretion system and selected lipids (i.e., phthiocerol dimycocerosates) are required for communication of *M. tuberculosis* with the host cytosol (Simeone et al., 2016; Augenstreich et al., 2017), with subsequent detection of bacterial DNA by cytosolic sensors, and mitochondrial stress (Wiens and Ernst, 2016). This process leads to a cascade of innate immune signaling events (Collins et al., 2015; Wassermann et al., 2015; Watson et al., 2015), including reinforced AIM-2 (Absence in Melanoma 2) and NLRP3 inflammasome activation, increased interleukin-1β (IL-1β) and/or IL-18 secretion (Dorhoi et al., 2012; Kupz et al., 2016; Wong and Jacobs, 2011) and activation of the cyclic GMP-AMP synthase (cGas)/Stimulator of Interferon Genes (STING)/TANK-binding kinase 1 (TBK1)/IRF3 axis. The latter signaling cascade results in the production of type I interferons (IFNs) (Stanley et al., 2007). Apart from innate immune activation, secreted ESX-1 effectors also induce specific host Th1 cell

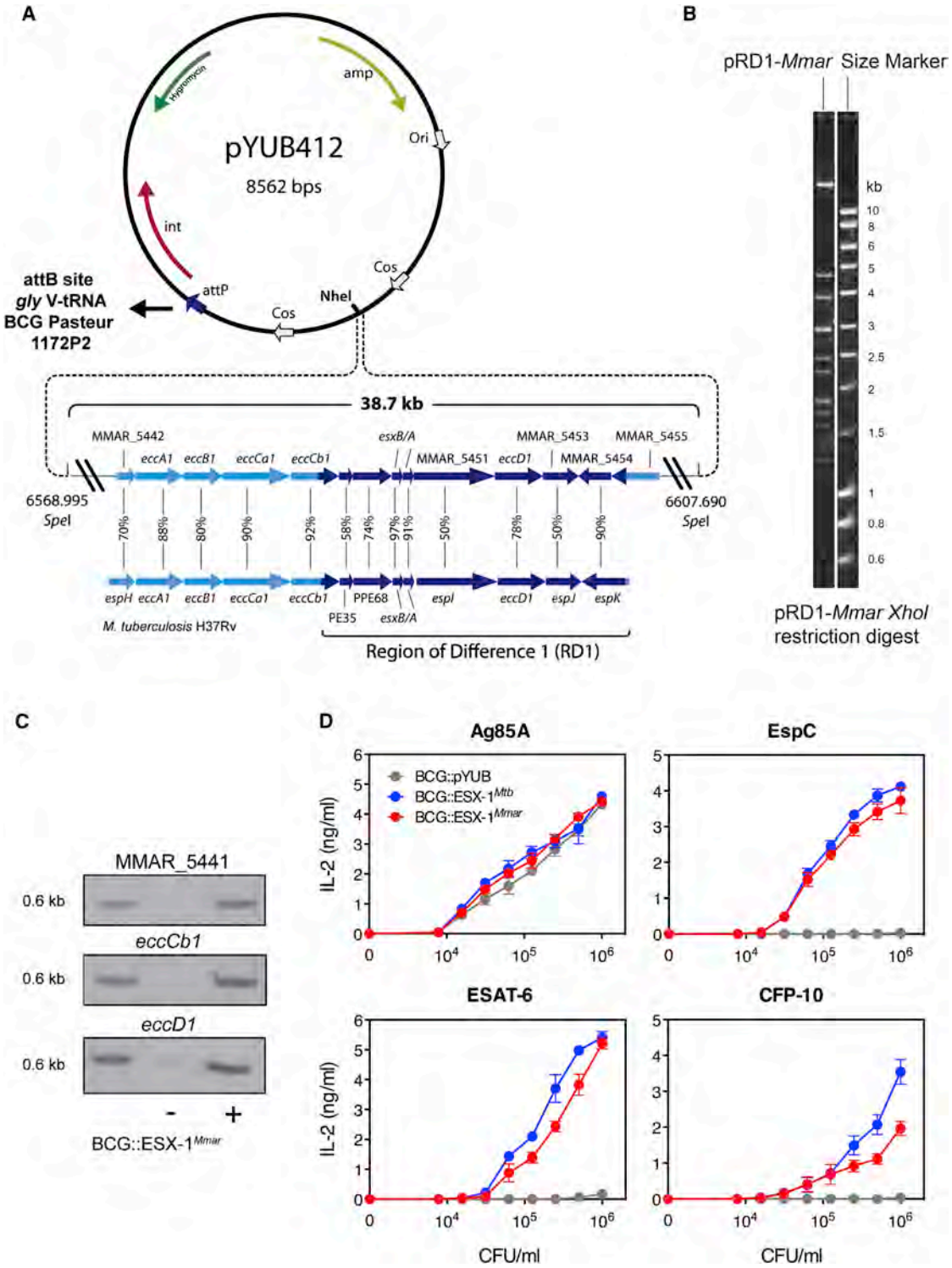

Figure 1. Stable Genetic Complementation of BCG Pasteur Integrating the *esx-1* Region of *M. marinum*

(A) Schematic representation of the integrating vector (Bange et al., 1999), the *Nhe*I cloning site, and the 38.7-kb insert from *M. marinum* M containing the *esx-1* locus. Amino acid sequence identities between gene products in the orthologous *esx-1* loci of *M. marinum* and *M. tuberculosis* are depicted in percentages.

(B) PCR-based verification of the integration of the *esx-1* locus into BCG::ESX-1^{Mmar}, using several primers spanning the *esx-1* locus of *M. marinum* and negative and positive DNA controls.

(C) Ethidium-bromid stained fragments of *Xho*I restriction digest of pRD1-*Mmar*, separated by agarose gel electrophoresis.

(legend continued on next page)

responses with strong protective potential (Brodin et al., 2004, 2006). Early attempts to improve the protective efficacy of BCG by heterologously expressing ESX-1 from *M. tuberculosis*, a biosafety level (BSL) 3 organism, produced mixed results. Vaccine efficacy was improved (Pym et al., 2003), but as a side effect virulence was increased (Pym et al., 2002), making this recombinant BCG strain likely too virulent as to be used for vaccine applications. Thus, the rationale emerged to express the ESX-1 systems of related but less pathogenic mycobacteria in BCG. *M. tuberculosis* H37Rv and *M. marinum*, a BSL2 aquatic mycobacterium that can infect fish or frogs and occasionally causes skin infections in humans, share a substantial core genome, with high amino acid sequence conservation, particularly across the genes encoding the ESX-1 system (Figure 1A). Here, we engineered a recombinant BCG candidate vaccine that harbored the *esx-1* locus of *M. marinum* (BCG::ESX-1^{Mmar}). We then interrogated the biological and immunological consequences of this heterologous ESX-1^{Mmar} expression in the context of vaccination. Using different murine infection models, we identified previously undiscovered immunological features of recombinant BCG linked to cytosolic pattern recognition and we provide compelling evidence of significantly improved protective vaccine efficacy.

RESULTS

Construction of the Recombinant BCG ESX-1^{Mmar}-Proficient Strain

An *esx-1* locus-containing clone was selected from a Bacterial Artificial Chromosome (BAC) library of *M. marinum* reference strain M. This library was originally constructed to scaffold and validate the whole-genome sequence assembly of this strain (Stinear et al., 2008). The BAC clone was used as substrate for sub-cloning a 38.7-kb-sized fragment into the integrating cosmid vector pYUB412 (Bange et al., 1999) (Figures 1A and 1B). Sequence analysis revealed that the cloned fragment carried a nucleotide deletion in the *eccCb*$_1$ gene (6 C instead of 7 C in the published genome sequence [Stinear et al., 2008] GenBank CP000854 at position 6589,378-84) (Figure S1), causing a frameshift in EccCb$_1$. Further analysis showed that the same *eccCb*$_1$ nucleotide deletion was present in the genome of the M strain (M^{Pasteur}), used for construction of the BAC library (Figure S1). This finding likely explains the previously reported differences in ESAT-6 secretion and virulence between the attenuated *M. marinum* M^{VU} variant and other *M. marinum* M variants used in diverse laboratories (Abdallah et al., 2009; Hagedorn et al., 2009; Ramakrishnan et al., 2000; Simeone et al., 2012), as the *M. marinum* M^{VU} also harbors this mutation. The frameshift in the cosmid was repaired using a phage lambda Red recombineering approach (Chaveroche et al., 2000). We then transformed the ESX-1-repaired cosmid into BCG Pasteur 1173P2 (Figure 1C). Comparison of the in vitro growth characteristics of the obtained recombinant BCG::ESX-1^{Mmar} strain showed that they were similar to other BCG strains (Figure S2A).

The Heterologous ESX-1 System Is Functional in the BCG::ESX-1^{Mmar}

The main secreted *M. tuberculosis* ESX-1 effectors ESAT-6 and CFP-10 share very high amino acid sequence identity with their *M. marinum* orthologs (Figure S2B), so we assessed the functionality of the heterologous ESX-1^{Mmar} secretion machinery by using major histocompatibility complex (MHC)-II-restricted T cell hybridomas specific to different ESX-1 effectors. In this model, presentation of ESX-1 effectors is dependent on their proper secretion (Frigui et al., 2008). BCG::ESX-1^{Mmar}-infected bone-marrow-derived dendritic cells (BM-DCs) presented ESAT-6^{Mmar} and CFP-10^{Mmar} to specific T cell hybridomas in a manner indistinguishable from BCG::ESX-1^{Mtb}-infected BM-DCs (Figure 1D). Similarly, EspC (Rv3615c), an ESX-1-secretion-associated protein that forms secretion-needle-like structures (Ates and Brosch, 2017; Lou et al., 2017), and is exported in a co-dependent way with ESAT-6 (MacGurn et al., 2005), was efficiently presented by BM-DCs infected with either BCG::ESX-1^{Mmar} and BCG::ESX-1^{Mtb} (Figure 1D). All tested BCG strains induced the antigenic presentation of the control antigen Ag85A, secreted by the Twin-Arginine Translocation (TAT) pathway (Figure 1D). These data confirmed the functionality of the heterologous *M. marinum* ESX-1 system in BCG::ESX-1^{Mmar}, including the successful interaction with the *trans*-acting EspACD proteins of BCG that are encoded outside the cosmid-contained *M. marinum* fragment.

BCG::ESX-1^{Mmar} Shows Reduced Virulence Compared to BCG::ESX-1^{Mtb}

We next compared in vivo growth in severe combined immunodeficient (SCID) mice of BCG::ESX-1^{Mmar} with *M. tuberculosis* H37Rv, BCG::ESX-1^{Mtb} and parental BCG Pasteur. In this model in which weight loss is an index of disease development, BCG::ESX-1^{Mmar} induced a weight-loss curve similar to BCG Pasteur (Figures 2A and 2B). In contrast, mice infected with *M. tuberculosis* H37Rv or BCG::ESX-1^{Mtb} lost 20% of their weight significantly earlier, indicating that BCG::ESX-1^{Mmar} is more attenuated than BCG::ESX-1^{Mtb} (Pym et al., 2002, 2003).

BCG::ESX-1^{Mmar} Modulates the Host Innate Immune Response via Phagosomal Rupture

To determine further ESX-1^{Mmar}-associated biological consequences, we first confirmed that BCG::ESX-1^{Mmar} induced phenotypic and functional maturation of DC in a similar manner as control strains (BCG::pYUB, BCG::ESX-1^{Mtb} and wild-type (WT) *M. tuberculosis* H37Rv). This effect was evaluated by the upregulation of the CD40, CD80, and CD86 co-stimulatory molecules, modulation of MHC-I/II expression (Figure S3A), and production

(D) Demonstration of secretion of different ESX-1 substrates by BCG::ESX-1^{Mmar} strain through antigenic presentation by infected phagocytes. MHC-II-restricted antigenic presentation of ESAT-6, EspC and CFP-10 by BM-DCs generated from C57BL/6 (H-2^b) or C3H (H-2^k) mice, infected in vitro by different BCG strains, to T cell hybridomas; NB11 (specific to ESAT-6:1-20, restricted by I-A^b), IF1 (specific to EspC:40-54, restricted by I-A^b) or XE12 (specific to CFP-10:11-25, restricted by I-A^k), respectively. In this assay, the efficacy of antigenic presentation, evaluated by T cell activation and IL-2 production, is proportional to the amounts of ESX-1 secreted substrate. The DE10 hybridoma (specific to Ag85A:241-260, restricted by I-A^b) was used as a positive control. Error bars represent SD. The results are representative at least of two independent experiments.

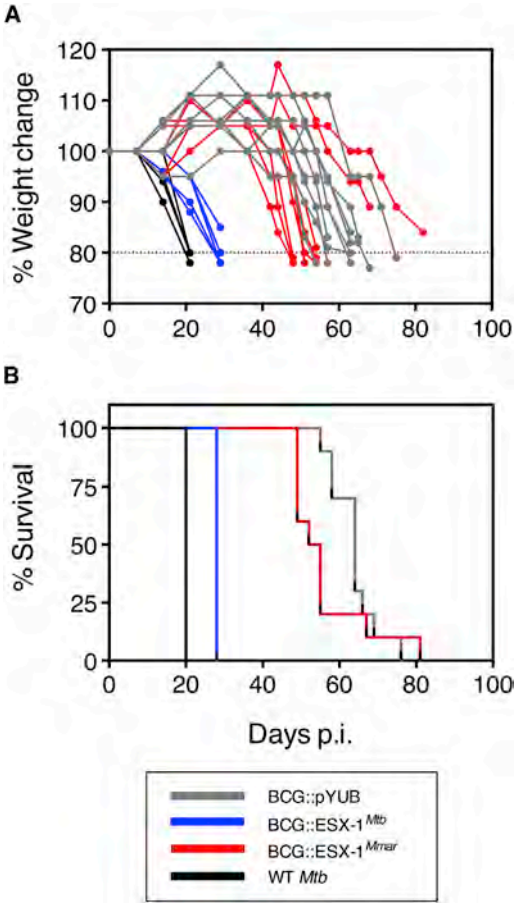

Figure 2. Attenuated Virulence of BCG::ESX-1^{Mmar} Strain, as Evaluated in Immunocompromised Mice

(A and B) SCID mice (n = 10 per group) were infected intravenously (i.v.) with 1 × 10^6 colony-forming units (CFUs)/mouse of different recombinant BCG strains in order to monitor the percentage of their weight change (A) and the survival (B) compared to *M. tuberculosis* H37Rv (WT *Mtb*). Mice were killed when reaching the humane endpoint, defined as the loss of >20% of body-weight in accordance with ethics committee guidelines. The obtained median survival times for groups of SCID mice were the following: *Mtb* WT 20 d; BCG::ESX-1^{Mtb} 28 days; BCG::ESX-1^{Mmar} 53.5 days; BCG Pasteur 64 days. Statistical analyses using the log-rank (Mantel-Cox) test performed with GraphPad Prism showed that the differences in survival between groups of animals infected with BCG::ESX-1^{Mmar} and *Mtb* WT or BCG::ESX-1^{Mtb} were highly statistically significant (****$p < 0.0001$), whereas for BCG::ESX-1^{Mmar} versus BCG Pasteur no significant difference was obtained ($p = 0.2136$). In contrast, median survival times for BCG::ESX-1^{Mtb} versus BCG Pasteur were highly statistically significant.

of pro/anti-inflammatory cytokines and chemokines (Figure S3B). As selected ESX-1-proficient mycobacteria such as *M. marinum*, *M. kansasii*, or *M. tuberculosis* (Simeone et al., 2012; Stamm et al., 2003; Wang et al., 2015) have been shown to induce ESX-1-mediated phagosome-to-cytosol communication, we explored whether BCG::ESX-1^{Mmar} was able to induce phagosomal rupture in host phagocytes. We used a flow-cytometric fluorescence resonance energy transfer (FRET) approach based on a green-to-blue fluorescence shift following cleavage of cytosolic coumarin-cephalosporin-fluorescein 4 (CCF4) by endogenous mycobacterial β-lactamase (Simeone et al., 2015). Analysis of infected human THP-1 macrophages revealed that BCG::ESX-1^{Mmar} induced a solid blue shift, implying contact with the host cytosol, albeit to a lesser degree compared to *M. tuberculosis* H37Rv and BCG::ESX-1^{Mtb} (Figure 3A). In contrast, the ESX-1-deficient negative control BCG strain did not induce a blue shift in the infected cells (Figure 3A).

Infection of WT THP-1 macrophage-like cells with BCG::ESX-1^{Mmar} or control strains showed that BCG::ESX-1^{Mmar} and BCG::ESX-1^{Mtb} both induced IFN-β production, although at a lower level than WT *M. tuberculosis*. In comparison, IFN-β secretion was not detected in BCG::pYUB and *M. tuberculosis* ΔESX-1 (Figure 3B). Infection of THP-1 cells deficient in either cGAS or STING, revealed that neither BCG nor *M. tuberculosis* (either WT or recombinant) led to IFN-β release (Figure 3C). As a functional control, we showed that cGAS or STING-deficient THP-1 cells released tumor necrosis factor-α (TNF-α)-like WT (Figure 3C). These data support our contention that a type I IFN response by ESX-1-proficient BCG strains depends on cytosolic exposure of mycobacterial DNA to then associate with cGAS.

In parallel, we found that infection with BCG::ESX-1^{Mmar}, BCG::ESX-1^{Mtb} or WT *M. tuberculosis*, significantly enhanced release of active IL-1β, compared to BCG::pYUB and *M. tuberculosis* ΔESX-1 (Figure 3B). These data are in agreement with earlier studies, which revealed that the release of active IL-1β is partially dependent on the interaction of mycobacterial DNA with AIM2 (Saiga et al., 2015).

Since ESX-1-dependent activation of STING has been reported to increase autophagy (Watson et al., 2012), we tested whether the BCG::ESX-1^{Mmar} or BCG::ESX-1^{Mtb} increased the presence of the cytosolic autophagy effector microtubule-associated protein 1A/1B-light chain 3 (LC3)-II. Using a flow-cytometry-based assay, we observed increased LC3-II accumulation in THP-1 cells infected with ESX-1-proficient recombinant BCGs relative to BCG::pYUB-infected cells (Figure S4A), without notable differences in cell mortality (Figure S4B). However, the observed differences between BCG WT and recombinant strains remained relatively small, in concordance with previous studies using western blotting or confocal microscopy (Romagnoli et al., 2012; Watson et al., 2012) (Figure S4A).

BCG::ESX-1^{Mmar} Induces Potent Polyfunctional Th1 Cell Responses against ESX-1-Secreted Antigens

Protection against TB largely depends on the host's ability to generate potent Th1 cell responses against mycobacterial protective antigens (Majlessi et al., 2015). C57BL/6 (H-2^b) or C3H (H-2^k) mice, immunized subcutaneously (s.c.) with BCG::ESX-1^{Mmar}, mounted IFN-γ T cell responses against *esx-1*-encoded ESAT-6 and CFP-10 antigens as well as ESX-1-secretion-associated EspC (Figures S5). These responses were similar to those detected in the BCG::ESX-1^{Mtb}- or WT *M. tuberculosis*-immunized groups. BCG::ESX-1^{Mmar}-immunized mice also displayed IFN-γ T cell responses against non-ESX-1-associated antigens shared with BCG that were comparable to those induced by the BCG::pYUB control, as exemplified by Ag85A-, PE19-, or PPE25-specific IFN-γ release (Figure S5A).

In-depth characterization of the functional Th1 subsets by intracellular cytokine staining (ICS) (Figures 4A, S6, and S7) showed

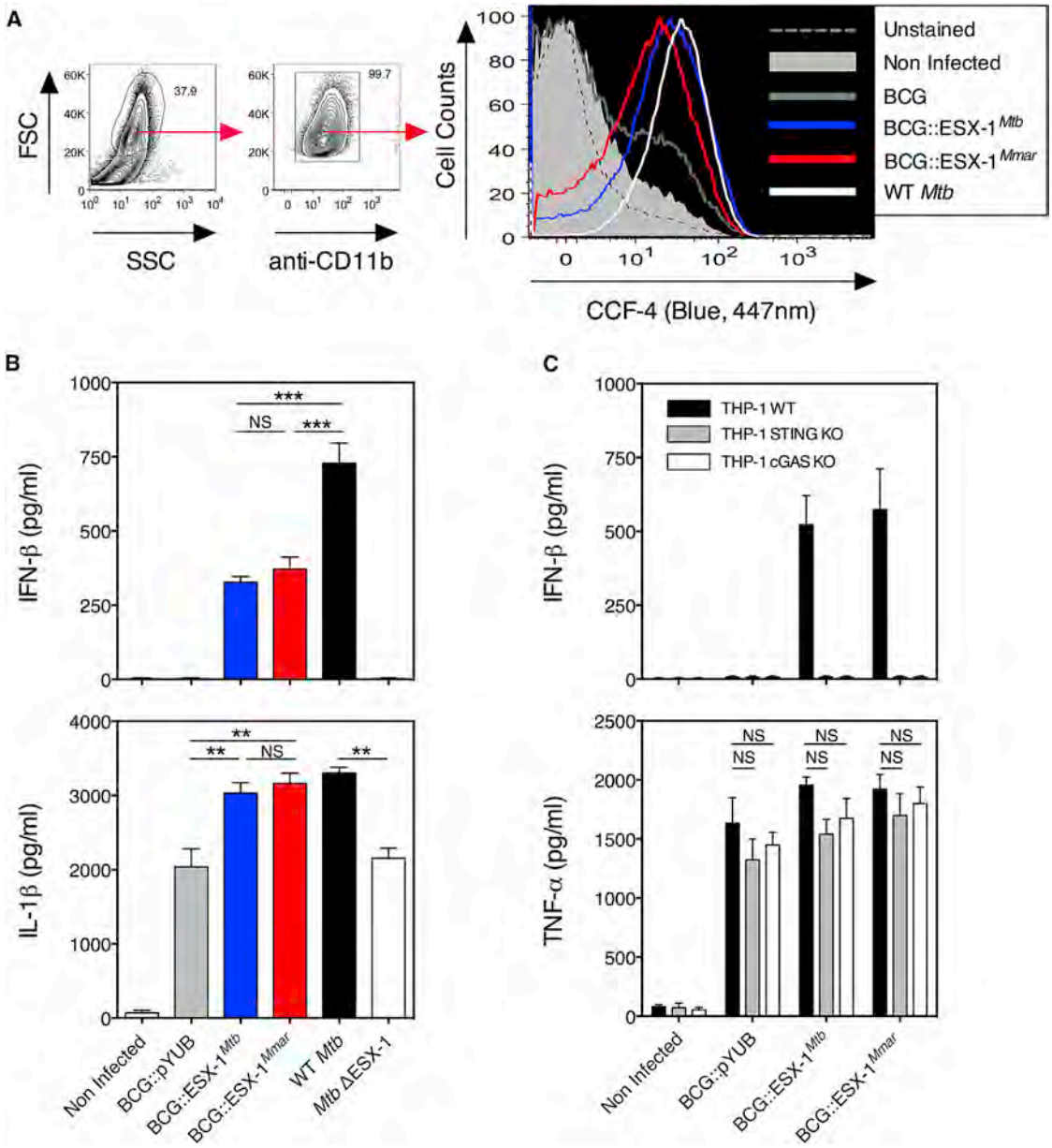

Figure 3. Dynamic Effects of Functional ESX-1 Secretion System of BCG::ESX-1^{Mmar} on the Host Innate Immune Responses

(A) Gating strategy and results of phagosomal rupture assay in WT THP-1 human macrophages, infected with different recombinant BCG strains, as detected at day 3 post-infection by CCF-4 FRET-based cytometry, compared to controls (Sayes et al., 2016).

(B and C) ELISA-based quantification of IFN-β and IL-1β (B), or IFN-β and TNF-α (C) contents in the culture supernatants of the infected WT or mutant THP-1 cells at 24 hr post-infection. The results are representative of two independent experiments. NS, not significant, ** or ***, statistically significant, as determined by one-way ANOVA test with Tukey's correction, with $p < 0.005$ or $p < 0.001$, respectively. Error bars indicate SD levels.

that BCG::ESX-1^{Mmar}, BCG::ESX-1^{Mtb}, as well as BCG::pYUB, all induced comparable percentages of Th1 cytokine-producing cells and similar compositions in single-, double-, and triple-Th1 cytokine producing cells, specific to the antigens present in BCG, i.e., Ag85A (Figure 4B) and PE19 or PPE25 (Figure S7A). In addition, BCG::ESX-1^{Mmar} and BCG::ESX-1^{Mtb} induced similar ESAT-6- or EspC-specific Th1 responses (Figure 4B). Indeed, the total percentage of Th1 cytokine-producing cells per mouse against these antigens was comparable among the mice immunized with the two ESX-1-proficient recombinant BCG strains (Figure S7). The responses were dominated by IL-2$^+$ TNF-α$^+$ and TNF-α$^+$ IFN-γ$^+$ double-positive and IL-2$^+$ TNF-α$^+$ IFN-γ$^+$ triple-positive CD4$^+$ T cells. Furthermore, the amount of Th1 cytokines produced by ESAT-6 specific CD4$^+$ T cell subsets in response to BCG::ESX-1^{Mmar} and BCG::ESX-1^{Mtb} were comparable (Figure 4C).

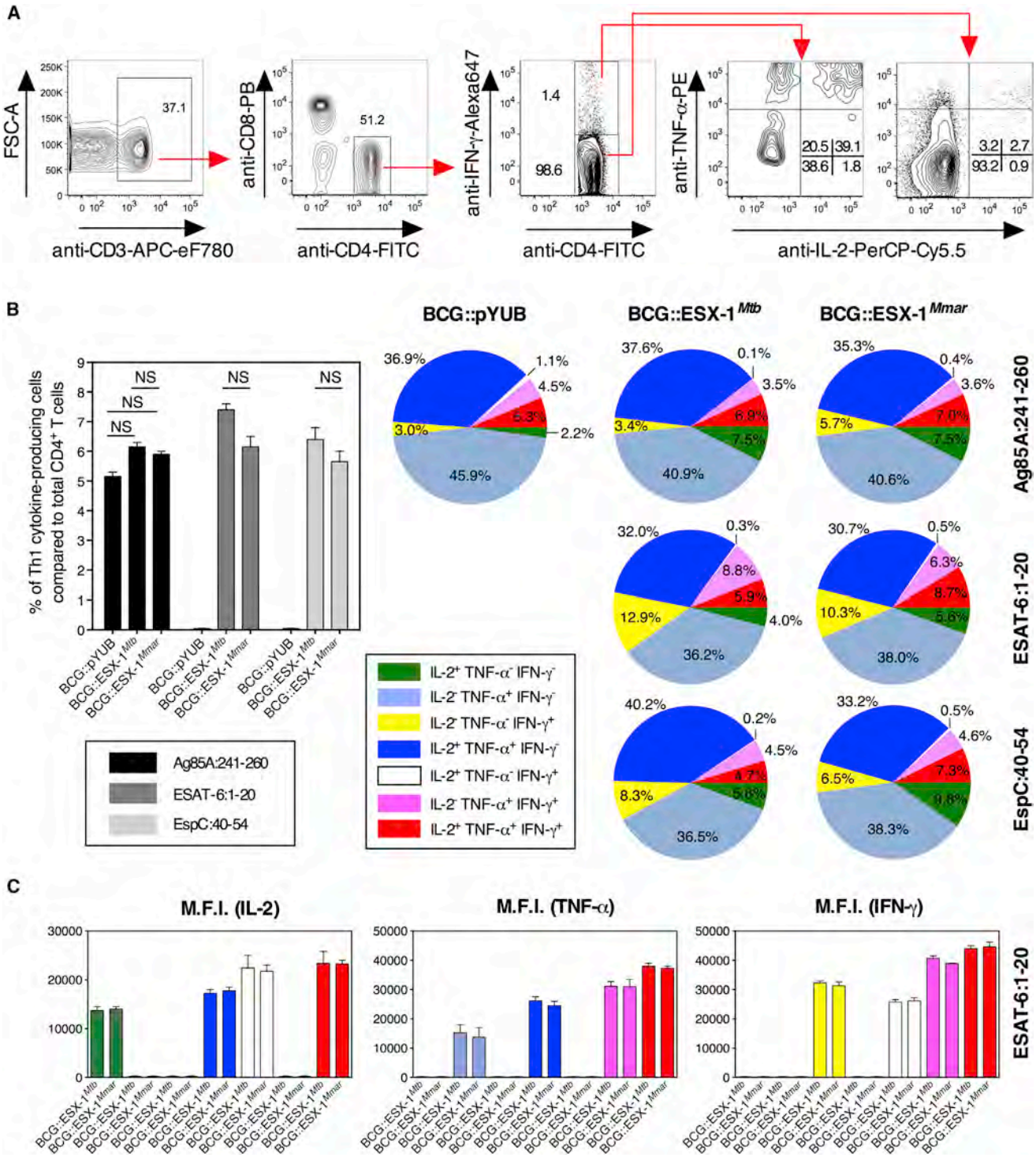

Figure 4. Dissection of Th1 Cell Responses Induced by BCG::ESX-1^{Mmar} Immunization

(A) Gating strategy adopted to detect different functional subsets of specific Th1 effectors in the spleen of BCG::ESX-1^{Mmar}-immunized C57BL/6 mice using ICS. Cytometric plots represent 5% contours, representative of three mice per group. Shown are cultures of splenocytes stimulated by ESAT-6:1-20.

(B) Percentages of antigen-specific Th1 cytokine producing T cells compared to total CD4$^+$ T splenocytes (left) and composition of Th1 cytokine-producing functional CD4$^+$ T cells, specific to different mycobacterial antigens, at 28 days post-immunization. Total splenocytes from each group were stimulated in vitro with 10 μg/mL of different synthetic peptides containing I-A^b-restricted immunodominant epitopes, prior to ICS, in order to determine frequencies of

(legend continued on next page)

BCG::ESX-1^{Mmar} Boosts Initiation of Anti-Mycobacterial Host CD8$^+$ T Cell Immunity

Independent lines of evidence point to a major role of CD8$^+$ T cells in anti-mycobacterial protection (Behar, 2013; Ryan et al., 2009). To evaluate the impact of BCG complementation with ESX-1, we immunized C3H (H-2^k) mice that specifically recognize a MHC-I-restricted CFP-10:32-39 epitope (Kamath et al., 2004) and found that the mice mounted CD8$^+$ T cell responses against CFP-10, as detected by IFN-γ production subsequent to stimulation of splenocytes with the peptide (Figure 5A). In addition, higher percentages of TNF-α^+ IFN-γ^+ bi-functional CD8$^+$ T cells specific to Ag85A:144-152 (Denis et al., 1998), TB10.4:20-28 (Majlessi et al., 2003), or PPE26: 44-52- (Sayes et al., 2012) MHC-I-restricted epitope were detected in the spleen of BCG::ESX-1^{Mmar}- or BCG::ESX-1^{Mtb}-immunized BALB/c (H-2^d) mice, relative to their BCG-immunized counterparts (Figure 5B). The increase in CD8$^+$ T cell responses against non-ESX-1-secreted antigens upon immunization with ESX-1-proficient BCGs supports the notion that ESX-1-mediated phagosomal rupture facilitates cross-presentation of mycobacterial antigens either due to type I IFN production (Le Bon et al., 2003) or by enhanced access of antigens to the cytosolic presentation machinery (van der Wel et al., 2007). The potentially increased persistence of ESX-1-proficient BCGs in the vaccinated host may also contribute to sustained availability of mycobacterial antigens required for the initiation of robust CD8$^+$ T cell effectors (Woodworth et al., 2008).

BCG::ESX-1^{Mmar} Protects Mice from TB Better than Standard BCG Vaccines

To assess the protective efficacy of the BCG::ESX-1^{Mmar} as a potential vaccine candidate, we immunized s.c. groups of C57BL/6 mice (n = 5 per group) with the different BCG strains. After 4 weeks, mice were challenged with *M. tuberculosis* H37Rv via the aerosol route and mycobacterial loads were determined in lungs and spleen 4 weeks later (Figure 6A). Both BCG ESX-1-proficient strains were superior to BCG Danish 1331, the model control BCG strain used in TB vaccine research, or BCG::pYUB in protecting against an *M. tuberculosis* H37Rv challenge both in the lungs and in spleen (Figures 6B and 6C) in this model. These data suggest that BCG::ESX-1^{Mmar} and BCG::ESX-1^{Mtb} show similar protective efficacies that are, in turn, superior to the parental BCG strains.

To further explore its protective performance, BCG::ESX-1^{Mmar} was tested in an independent preclinical vaccine trial within the framework of the TBVAC2020 consortium, where potential TB vaccine candidates are compared head-to-head relative to BCG Danish 1331 (Figure 7A). BCG::ESX-1^{Mmar} showed significantly enhanced protection against a challenge with the highly virulent *M. tuberculosis* strain HN878 (Beijing family) (Figure 7B) and *M. tuberculosis* strain M2 from the Harleem family (Figure 7C), as evidenced by greatly reduced mycobacterial loads in the lungs and spleen, as well as decreased proportions of inflamed lung tissue (Figure 7D).

DISCUSSION

With millions of doses delivered across generations of humans around the world, BCG is perhaps the most well-known example of a live, attenuated vaccine and is still widely used today as no higher-performing alternatives have been licensed to date. Developed in the 1920s by Calmette and Guérin after long-term in vitro passaging of a virulent *Mycobacterium bovis* isolate that became irreversibly attenuated, vaccination with BCG of an estimated 3 billion individuals confirmed that BCG was safe in the immunocompetent host (Fine et al., 1999). Besides BCG, the other human anti-TB vaccine used at a larger scale is the vole-bacillus *Mycobacterium microti*. Different attenuated variants were successfully used to vaccinate 10,000 adolescents in the UK (Hart and Sutherland, 1977) and half a million babies in the former Czechoslovakia (Sula and Radkovský, 1976) in the 1960s.

However, reflection on the history of almost 100 years of human anti-TB vaccination shows that despite undeniable beneficial effects conferred to small children, vaccination with BCG or *M. microti* has been insufficient to prevent the current global re-emergence of TB. Interestingly, BCG and *M. microti* strains have one major genetic feature in common. They have independently deleted portions of the region of difference 1 (RD1) (Mahairas et al., 1996; Brodin et al., 2002), which in *M. tuberculosis* and many other mycobacteria encodes the ESX-1 type VII secretion system (Abdallah et al., 2007; Bottai et al., 2016; Gröschel et al., 2016). The biological basis for key ESX-1-mediated effects are primarily linked to the ESX-1-dependent induction of phagosome-cytosol communication (Simeone et al., 2012, 2015; van der Wel et al., 2007; Conrad et al., 2017). Indeed, mycobacterial cytosolic contact triggers a cascade of cellular signaling events that are of upmost importance for innate and adaptive immune responses. ESX-1-deficient BCG and *M. microti* vaccine strains are unable to initiate these responses (Gröschel et al., 2016; Majlessi and Brosch, 2015; Majlessi et al., 2015).

We reasoned that influencing phagosome biology through ESX-1 secretion might enhance the protective ability of BCG, and we wanted to uncouple the beneficial immunological ESX-1-mediated effects from the gain-of-virulence linked to the insertion of genes from a BSL3 organism into BCG. We thus heterologously expressed in BCG the ESX-1 from *M. marinum*, a mycobacterium that shares with BCG the BSL2 classification. Successful integration of the *M. marinum* ESX-1 locus was confirmed by PCR and use of a panel of ESX-1 antigen-specific T cell hybridomas. Interestingly, we detected lower antigenic presentation of CFP-10 by dendritic cells infected with BCG::ESX-1^{Mmar} compared to BCG::ESX-1^{Mtb}, which might reflect a lower CFP-10 antigen availability due to the

single-, double-, or triple-positive CD4$^+$ cells producing IL-2, TNF-α, and/or IFN-γ. NS, not significant as determined by one-way ANOVA test with Tukey's correction.

(C) The geometric mean fluorescence intensities (MFIs), proportional to the intracellular amounts of IL-2, TNF-α, or IFN-γ, in each of the ESAT-6-specific functional Th1 subsets, as determined in the spleen of mice immunized with BCG::ESX-1^{Mmar} or BCG::ESX-1^{Mtb}. Additional information is provided in Figures S6 and S7.

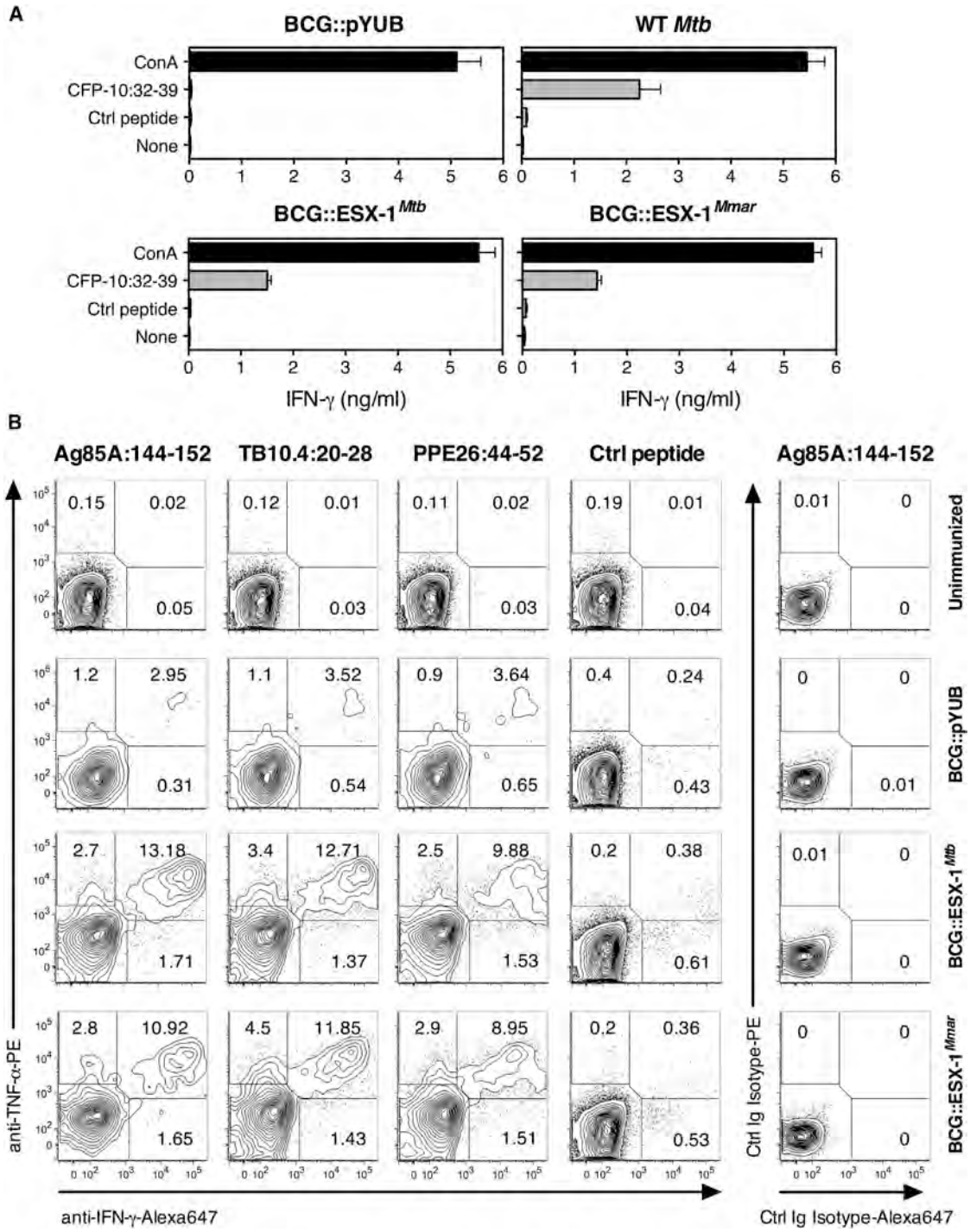

Figure 5. Enhanced Induction of Key CD8$^+$ T Cell Effectors by BCG::ESX-1^{Mmar} in Immunocompetent Mice

(A) T cell IFN-γ responses of C3H (H-2^k) mice (n = 3 per group) immunized s.c. with 1 × 10^6 CFUs/mouse of different BCG strains, as assessed at 4 weeks post-immunization. Pool of total splenocytes of the immunized mice were stimulated in vitro with synthetic MHC-I-restricted CFP-10-derived peptides during 72 hr. Error bars represent SD.

(B) Detection of TNF-α- and/or IFN-γ-producing CD3$^+$ CD4$^-$ CD8$^+$ T splenocytes by ICS applied on total splenocytes of BALB/c (H-2^d) mice (n = 3 per group), immunized s.c. with 1 × 10^6 CFUs/mouse of different BCG strains. At 5 weeks post-immunization, splenocytes were stimulated in vitro with MHC-I H-2K^d-restricted epitopes from Ag85A, TB10.4, PPE26, or the LCMV-NP:118-126 as a negative control peptide. In parallel, stimulated cells were stained with control immunoglobulin (Ig) isotypes. Cytometric plots represent 5% contours with outliers, representative of three mice per group. The results are representative of two independent experiments.

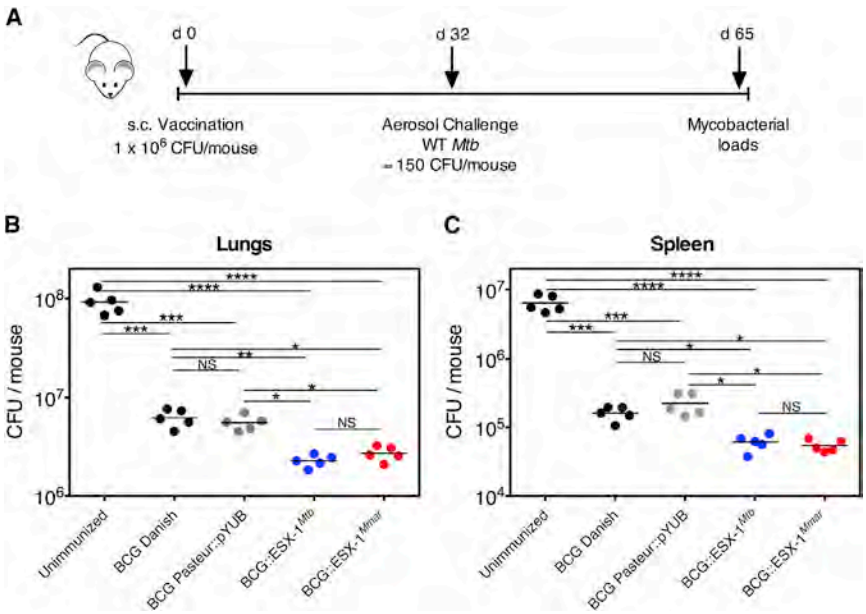

Figure 6. Improved Protection Potential of BCG::ESX-1^{Mmar} Strain Significantly Enhances Protective Capacity against an *M. tuberculosis* H37Rv Challenge in Mice

(A) Immunization protocol of mice adopted in order to evaluate protective capacity of different BCG strains.

(B and C) C57BL/6 mice (n = 5 per group) were left unimmunized or vaccinated s.c. with 1 × 10^6 CFUs/mouse of BCG Pasteur::pYUB, BCG Danish, BCG::ESX-1^{Mtb} or BCG::ESX-1^{Mmar} strain with ≈150 CFUs/mouse of *M. tuberculosis* H37Rv strain via aerosol route, as determined by CFU counting in the lungs day 1 post-infection. The mycobacterial loads in the lungs (B) and spleen (C) of individual mice were determined. NS, not significant, *, **, ***, ****, statistically significant, as determined by one-way ANOVA test with Tukey's correction, with $p < 0.05$, $p < 0.005$, $p < 0.001$, or $p < 0.0001$, respectively. Note that for these experiments a H37Rv *M. tuberculosis* strain was used that was passaged in the past in mice to maintain high virulence, and that the inoculum for the aerosol challenge was prepared from exponentially growing cultures.

heterologous expression of *M. marinum* proteins that need to cooperate for secretion with proteins from BCG.

The introduction of the ESX-1^{Mmar} region into BCG resulted in a minor, non-significant increase in virulence relative to parental BCG Pasteur and was greatly reduced compared to the virulence of BCG::ESX-1^{Mtb}. As the magnitude of phagosomal rupture by BCG::ESX-1^{Mmar} and BCG::ESX-1^{Mtb} was comparable, it suggests that phagosome escape is not the only determining factor that explains the virulence differences observed between ESX-1-proficient and ESX-1-deficient mycobacteria. Alternatively, the heterologous expression of a large DNA fragment from a more distantly related species with different host specificity, i.e., *M. marinum*, in BCG might reduce the in vivo fitness of the recombinant BCG::ESX-1^{Mmar}, although we observed similar in vitro growth characteristics to standard BCG.

We next evaluated the immunological repercussions of the ESX-1-introduction into BCG by analyzing innate immune responses, particularly in light of the most recent literature. IL-1β is protective in the context of *M. tuberculosis* infection (Fremond et al., 2007), and its catalytic cleavage is mediated by the NLRP3 inflammasome/caspase-1 pathway (Muruve et al., 2008). We showed that ESX-1-proficient BCGs mount a higher IL-1β response suggesting that cytosolic access of mycobacterial compounds promotes activation of the inflammasome. In addition to induction of IL-1 β, recent evidence points to a role for ESX-1-mediated cytosolic contact in NLRP3-inflammasome-mediated secretion of IL-18 by infected CD11c$^+$ immune cells (Kupz et al., 2016). This leads to non-cognate production of IFN-γ by *M. tuberculosis*-antigen-independent memory CD8$^+$ T cells and NK cells. Such IL-18-dependent and rapid IFN-γ responses are not induced by current anti-TB vaccines (Gengenbacher et al., 2016; Kupz et al., 2016). In this context, the rationale is strengthened for leveraging ESX-1 function as an important additional element in the design of third-generation vaccines and host-directed therapy against TB.

By acquiring cytosolic access, mycobacterial molecular fingerprints, such as extracellular DNA, can also be sensed by germline-encoded pattern recognition receptors in host cell such as AIM2 (Hornung et al., 2009; Saiga et al., 2015) or cGAS (Collins et al., 2015; Wassermann et al., 2015; Watson et al., 2015). We observed that the BCG::ESX-1 strains induced IFN-β mediated by the cGAS/STING pathway in human macrophages. We acknowledge that the role of type I IFNs in the context of *M. tuberculosis* infection is somewhat conflicted (McNab et al., 2015). Studies in humans (Berry et al., 2010) and in animal models report a detrimental role of type I IFNs during *M. tuberculosis* infection (Manca et al., 2005; Ordway et al., 2007; Stanley et al., 2007). A possible explanation is that IFN-α/β undermine inflammasome activation and associated host protective cytokines such as IL-1β (Guarda et al., 2011). However, this pro-bacterial role of type I IFNs during infection with *M. tuberculosis* could turn out to be pro-host during vaccination. While type I IFNs negatively regulate active IL-1β secretion during *M. tuberculosis* infection (Novikov et al., 2011), we observed both increased IL-1β and IFN-β production induced by the ESX-1-proficient BCG vaccine candidates. Therefore, if an activated cGas/STING/TBK1/IFR3/type I IFN pathway contributes to the persistence of attenuated vaccine strains and the activation of non-infected neighboring cells (Ablasser et al., 2013), this effect might favorably increase the spatial and temporal interplay between the vaccine and the host immune system, ultimately contributing to improved vaccine efficacy.

Apart from the prompt innate immune response, the late adaptive immune system plays a key role in anti-mycobacterial immunity (Orme et al., 2015). We found that the BCG::ESX-1^{Mmar} induces a potent Th1 cell response against strong immunogens exported by ESX-1, which enlarges the antigenic repertoire compared to the currently used BCG vaccine, and thus represents a desirable feature in the light of the incomplete protection conferred by BCG. The presence of polyfunctional

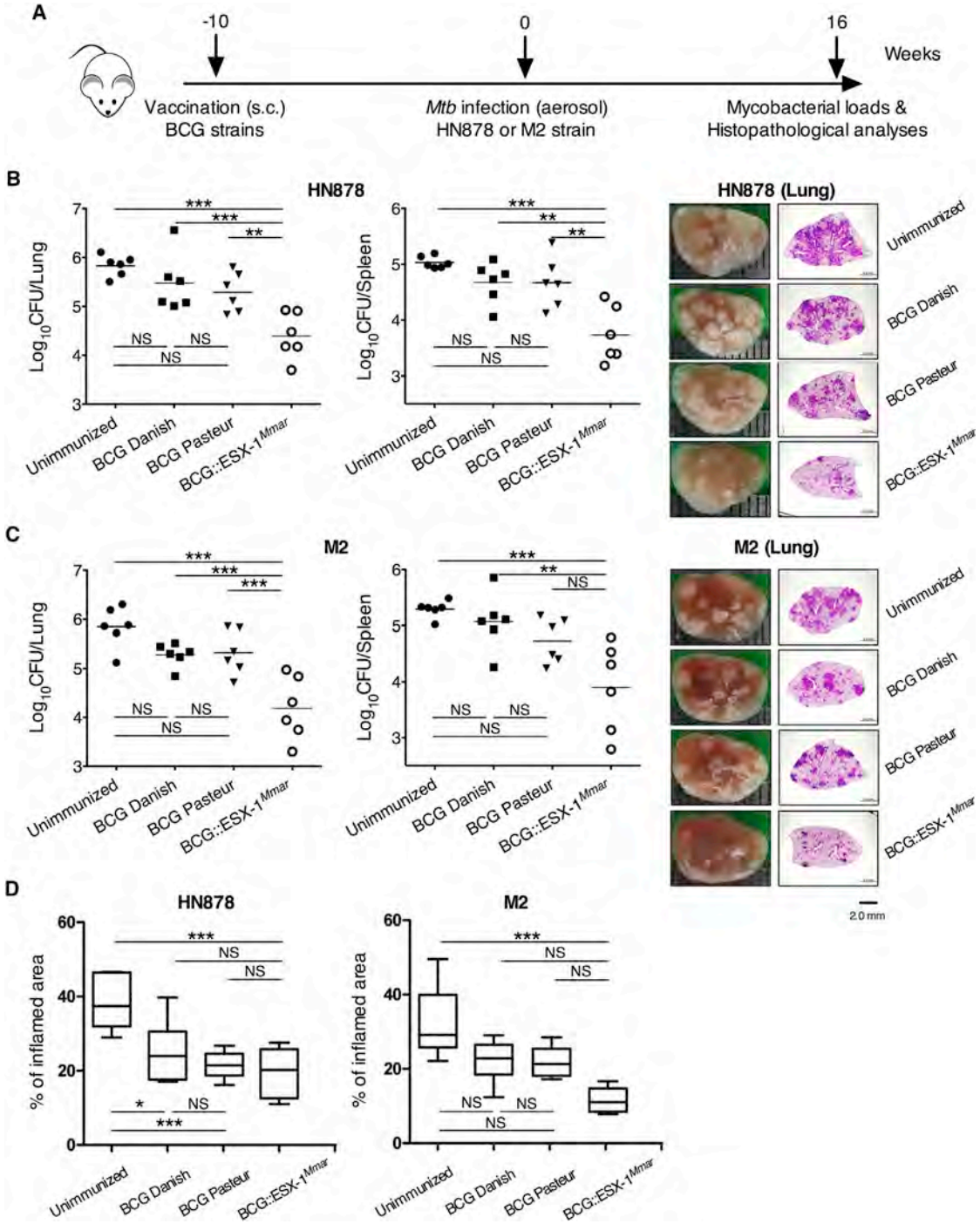

Figure 7. Improved Protection Potential of BCG::ESX-1^{Mmar} Strain Relative to Standard BCG Strains in Mice against a Challenge with Hypervirulent *M. tuberculosis* Strains HN878 and M2

(A) Immunization protocol with different BCG strains.

(B and C) Bacterial loads in the lungs and spleens 26 weeks post-immunization and 16 weeks after aerosol challenge with the *M. tuberculosis* HN878 (B) or M2 (C) strains. Mice were challenged with the *M. tuberculosis* HN878 strain (approximately 200 CFUs/mouse) or M2 strain (approximately 50–60 CFUs/mouse) via the aerosol route. The CFUs in the lungs and spleens of each group were analyzed by culturing lung and spleen homogenates and enumerating the bacteria. Note that CFU data shown correspond to counts that were obtained from the left-superior lobes of the lungs. The data are presented as the median ± interquartile range (IQR) $\log_{10}$ CFUs/organ (n = 6), and the levels of significance for comparisons between samples were determined by a one-way ANOVA, followed by Dunnett's multiple comparison test.

(legend continued on next page)

Th1 cytokine-producing cells against ESX-1-secreted antigens upon vaccination with the recombinant BCGs adds another convincing feature of the broadened T cell specificities. Apart from $CD4^+$ T cells, we detected improved $CD8^+$ T cell responses by analyzing functional $CD8^+$ T cells. This strong adaptive immune response could be partly explained by a bridging function of activated IFN-β between innate and adaptive immunity, as has been described for type I IFNs (Le Bon et al., 2003). Importantly, in addition to type I IFNs IL-1β and inflammasome activation also play roles in regulating the differentiation and function of $CD8^+$ T cells during *M. tuberculosis* infection (Booty et al., 2016). $CD8^+$ T cell effectors are primed through increased inflammasome signaling (IL-1β), in concert with the upregulation of chemo-attractants CCL2, CCL5, and CXCL10, of which we detected elevated levels (Figure S3B) (Le Bon et al., 2003; Sagoo et al., 2016). These data support a model where ESX-1-mediated cytosolic access assists presentation to and activation of the cytosolic presentation machinery through induction of type I IFNs (Le Bon et al., 2003) and potentially increased bacterial persistence (Woodworth et al., 2008).

The hypothesis that ESX-1-mediated cytosolic access improves the performance of recombinant BCG through enhanced innate immune signaling and enlarged antigenic repertoire is supported by our results from the mouse models where BCG::ESX-1^{Mmar} showed superior protective efficacy compared to parental BCG. These results are in accord with those obtained using an attenuated *M. tuberculosis* strain that lacks the characteristic *esx-5*-associated *pe/ppe* genes, but harbors all other components of the ESX-5 system, as well as an intact ESX-1 system (Sayes et al., 2012). Like BCG::ESX-1^{Mmar}, this strain named *MtbΔppe25-pe19* is able to induce innate immune responses linked to cytosolic pattern recognition and shows significantly improved protection against an *M. tuberculosis* challenge in a mouse infection model (Sayes et al., 2016). These results suggest that, despite the different genetic background and the different origin of the ESX-1 system, ESX-1-mediated functions are essential for increasing protection levels above those provided by vaccination with standard BCG strains.

In conclusion, the heterologous expression of an *M. marinum*-derived ESX-1 system in BCG yielded a recombinant vaccine candidate with relatively low virulence levels in SCID mice, which are comparable with those of other BCG strains (Zhang et al., 2016), and a capacity to induce selected innate and adaptive immune responses that depend on phagosome-cytosol communication in the host phagocyte. Such responses are not induced by first-generation anti-TB vaccines such as BCG or *M. microti* and might as well not be induced by the second-generation anti-TB vaccine candidates that have recently entered clinical development (Kupz et al., 2016). Given that 90%–95% of *M. tuberculosis* exposed individuals do not develop active TB disease during their lifetime, host immune effectors are largely capable of inducing protective immunity (Ottenhoff and Kaufmann, 2012). We propose that a virulence-attenuated, ESX-1-proficient BCG vaccine might be best able to mimic the natural route of infection and induce the "correct" phagosomal biology, leading to protective immunity at the same points of host-pathogen contact as *M. tuberculosis*. We argue that this important biological feature should not be left out from the rational design of third-generation vaccines, giving BCG::ESX-1^{Mmar} a clear potential to better control TB.

EXPERIMENTAL PROCEDURES

Mycobacterial Strains and Preparation of Recombinant Strains

Mycobacterial strains included the *M. tuberculosis* strains H37Rv (stocks held at Institut Pasteur, Paris), HN878 and M2 (ITRC, Changwon), as well as the BCG strains Pasteur 1173P2 and Danish 1331. Recombinant strains were obtained by transformation with the pRD1-2F9 cosmid (Pym et al., 2002) and the pESX-1^{Mmar} cosmid described in detail in the Supplemental Information.

Antigen-Presenting Assay

Several MHC-II-restricted T cell hybridomas specific to mycobacterial antigens were used in order to detect the secretion by mycobacteria, which leads to the antigenic presentation by the infected BM-DCs of different ESX-1 substrates, as described in detail in the Supplemental Information.

ELISA and Multiplex Cytokine and Chemokine Assays and FRET Assays

Levels of various cytokines and chemokines in BM-DC culture supernatants were determined by multiple ProcartaPlex (Affymetrix) kit assays and a Luminex X-100 Reader (Supplemental Information). For FRET analyses a recently described protocol (Simeone et al., 2015) was used with THP-1 cells to detect fluorescence emission changes from green (535 nm) to blue (447 nm) induced by β-lactamase-mediated cleavage of coumarin-cephalosporin-fluorescein (CCF-4) (Supplemental Information).

Immunogenicity and T Cell Assay and T Cell Intracellular Th1 Cytokine Assay

For immunological studies splenocytes from immunized C3H and C57BL/6 mice (Janvier) were cultured in 24- or 96-well plates in the presence of various mycobacterial antigens, followed by ELISA-mediated quantification of IFN-γ and/or flow-cytometric analysis (described in detail in the Supplemental Information).

In Vivo Experiments

Studies in immunocompetent and immunodeficient mice were performed according to European and French guidelines (Directive 86/609/CEE and Decree 87–848 of 19 October 1987) after approval by the Institut Pasteur Safety, Animal Care and Use Committee (Protocol 11.245) and local ethical committees (CETEA 2012–0005 and CETEA 2013–0036). In addition, independent vaccine efficacy studies involving *M. tuberculosis* HN878 and M2 challenges were performed in accordance with Korean Food and Drug Administration (KFDA) guidelines and approved by the Ethics Committee and Institutional Animal Care and Use Committee (Permit Number: 2015-0274) of the Laboratory Animal Research Center at Yonsei University College of Medicine (Seoul, Korea). More details on these experiments are described in the Supplemental Information.

Statistical Analyses

For statistical analyses, GraphPad Prism software (GraphPad) was used as described in detail in the Supplemental Information.

(D) Lung samples collected for histopathology were preserved overnight in 10% normal buffered formalin, embedded with paraffin, sliced into 4- to 5-μm-thick sections, and stained with H&E. The superior lobes of the right lung were stained with H&E to assess the severity of inflammation. The level of inflammation in the lungs was evaluated using ImageJ software (NIH). Percentages of the inflamed areas are presented as whisker boxplots (whiskers represent minimum and maximum values) (n = 6), and a one-way ANOVA followed by Dunnett's test was used to determine the significance of the findings.

ACCESSION NUMBERS

The accession number for selected flow-cytometric data reported in this paper is Flow Repository: FR-FCM-ZY24 (https://flowrepository.org/id/FR-FCM-ZY24).

SUPPLEMENTAL INFORMATION

Supplemental Information includes Supplemental Experimental Procedures and six figures and can be found with this article online at http://dx.doi.org/10.1016/j.celrep.2017.02.057.

AUTHOR CONTRIBUTIONS

Conceptualization, M.I.G., F.S., S.J.S., W.F., S.-N.C., L.M., and R.B.; Investigation, M.I.G., F.S., S.J.S., W.F., A.P., N.H., R.C., R.S., L.M., and R.B.; Formal Analysis, M.I.G., F.S., M.O., W.B., L.M., and R.B; Writing – Review & Editing, M.I.G., F.S., S.J.S., T.S.v.d.W., L.M., and R.B.

ACKNOWLEDGMENTS

We thank Veit Hornung (University of Munich) for kindly providing cGAS and STING K.O. cell lines; Peter Sebo (Czech Academy of Sciences, Prague) for ESAT-6 and CFP-10 proteins, Jean-Marc Ghigo for vector pKOBEG and advice, and Lalita Ramakrishnan, Thierry Soldati, and Timothy Stinear for *M. marinum* M strains. We are also grateful to Timothy Stinear for critically reading of the manuscript and advice. M.I.G. receives an MD/PhD scholarship and support from the Graduate School of Medical Sciences, both University of Groningen, the Netherlands. This study was in part supported by the European Union's Horizon 2020 Research and Innovation Program (grant 643381 TBVAC2020), the Agence National de Recherche (grants ANR-14-JAMR-001-02, ANR-14-CE-08-0017-04, ANR-10-LABX-62-IBEID), the Fondation pour la Recherche Médicale FRM (DEQ20130326471), and the Institut Pasteur (PTR441). This study was also supported by the International Research & Development Program through the National Research Foundation of Korea (NRF) funded by the Ministry of Science, ICT & Future Planning of Korea (NRF-2014K1A3A7A03075054). The mycobacterial construct BCG::ESX-1^{Mmar} has been patented under number PCT/EP2015/062457.

Received: December 6, 2016
Revised: January 18, 2017
Accepted: February 16, 2017
Published: March 14, 2017

REFERENCES

Abdallah, A.M., Gey van Pittius, N.C., Champion, P.A., Cox, J., Luirink, J., Vandenbroucke-Grauls, C.M., Appelmelk, B.J., and Bitter, W. (2007). Type VII secretion—mycobacteria show the way. Nat. Rev. Microbiol. *5*, 883–891.

Abdallah, A.M., Verboom, T., Weerdenburg, E.M., Gey van Pittius, N.C., Mahasha, P.W., Jiménez, C., Parra, M., Cadieux, N., Brennan, M.J., Appelmelk, B.J., and Bitter, W. (2009). PPE and PE_PGRS proteins of *Mycobacterium marinum* are transported via the type VII secretion system ESX-5. Mol. Microbiol. *73*, 329–340.

Ablasser, A., Schmid-Burgk, J.L., Hemmerling, I., Horvath, G.L., Schmidt, T., Latz, E., and Hornung, V. (2013). Cell intrinsic immunity spreads to bystander cells via the intercellular transfer of cGAMP. Nature *503*, 530–534.

Ates, L.S., and Brosch, R. (2017). Discovery of the type VII ESX-1 secretion needle? Mol. Microbiol. *103*, 7–12.

Augenstreich, J., Arbues, A., Simeone, R., Haanappel, E., Wegener, A., Sayes, F., Le Chevalier, F., Chalut, C., Malaga, W., Guilhot, C., et al. (2017). ESX-1 and phthiocerol dimycocerosates of *Mycobacterium tuberculosis* act in concert to cause phagosomal rupture and host cell apoptosis. Cell. Microbiol. http://dx.doi.org/10.1111/cmi.12726.

Bange, F.C., Collins, F.M., and Jacobs, W.R., Jr. (1999). Survival of mice infected with *Mycobacterium smegmatis* containing large DNA fragments from *Mycobacterium tuberculosis*. Tuber. Lung Dis. *79*, 171–180.

Behar, S.M. (2013). Antigen-specific CD8(+) T cells and protective immunity to tuberculosis. Adv. Exp. Med. Biol. *783*, 141–163.

Berry, M.P., Graham, C.M., McNab, F.W., Xu, Z., Bloch, S.A., Oni, T., Wilkinson, K.A., Banchereau, R., Skinner, J., Wilkinson, R.J., et al. (2010). An interferon-inducible neutrophil-driven blood transcriptional signature in human tuberculosis. Nature *466*, 973–977.

Booty, M.G., Nunes-Alves, C., Carpenter, S.M., Jayaraman, P., and Behar, S.M. (2016). Multiple inflammatory cytokines converge to regulate CD8+ T cell expansion and function during tuberculosis. J. Immunol. *196*, 1822–1831.

Bottai, D., Gröschel, M.I., and Brosch, R. (2016). Type VII secretion systems in Gram-positive bacteria. Curr. Top. Microbiol. Immunol. http://dx.doi.org/10.1007/82_2015_5015.

Brodin, P., Eiglmeier, K., Marmiesse, M., Billault, A., Garnier, T., Niemann, S., Cole, S.T., and Brosch, R. (2002). Bacterial artificial chromosome-based comparative genomic analysis identifies *Mycobacterium microti* as a natural ESAT-6 deletion mutant. Infect. Immun. *70*, 5568–5578.

Brodin, P., Majlessi, L., Brosch, R., Smith, D., Bancroft, G., Clark, S., Williams, A., Leclerc, C., and Cole, S.T. (2004). Enhanced protection against tuberculosis by vaccination with recombinant *Mycobacterium microti* vaccine that induces T cell immunity against region of difference 1 antigens. J. Infect. Dis. *190*, 115–122.

Brodin, P., Majlessi, L., Marsollier, L., de Jonge, M.I., Bottai, D., Demangel, C., Hinds, J., Neyrolles, O., Butcher, P.D., Leclerc, C., et al. (2006). Dissection of ESAT-6 system 1 of *Mycobacterium tuberculosis* and impact on immunogenicity and virulence. Infect. Immun. *74*, 88–98.

Chaveroche, M.K., Ghigo, J.M., and d'Enfert, C. (2000). A rapid method for efficient gene replacement in the filamentous fungus Aspergillus nidulans. Nucleic Acids Res. *28*, E97.

GBD 2013 Mortality and Causes of Death Collaborators (2015). Global, regional, and national age-sex specific all-cause and cause-specific mortality for 240 causes of death, 1990–2013: A systematic analysis for the Global Burden of Disease Study 2013. Lancet *385*, 117–171.

Collins, A.C., Cai, H., Li, T., Franco, L.H., Li, X.D., Nair, V.R., Scharn, C.R., Stamm, C.E., Levine, B., Chen, Z.J., and Shiloh, M.U. (2015). Cyclic GMP-AMP synthase is an innate immune DNA sensor for *Mycobacterium tuberculosis*. Cell Host Microbe *17*, 820–828.

Conrad, W.H., Osman, M.M., Shanahan, J.K., Chu, F., Takaki, K.K., Cameron, J., Hopkinson-Woolley, D., Brosch, R., and Ramakrishnan, L. (2017). Mycobacterial ESX-1 secretion system mediates host cell lysis through bacterium contact-dependent gross membrane disruptions. Proc. Natl. Acad. Sci. USA *114*, 1371–1376.

Denis, O., Tanghe, A., Palfliet, K., Jurion, F., van den Berg, T.P., Vanonckelen, A., Ooms, J., Saman, E., Ulmer, J.B., Content, J., and Huygen, K. (1998). Vaccination with plasmid DNA encoding mycobacterial antigen 85A stimulates a CD4+ and CD8+ T-cell epitopic repertoire broader than that stimulated by *Mycobacterium tuberculosis* H37Rv infection. Infect. Immun. *66*, 1527–1533.

Dorhoi, A., Nouailles, G., Jörg, S., Hagens, K., Heinemann, E., Pradl, L., Oberbeck-Müller, D., Duque-Correa, M.A., Reece, S.T., Ruland, J., et al. (2012). Activation of the NLRP3 inflammasome by *Mycobacterium tuberculosis* is uncoupled from susceptibility to active tuberculosis. Eur. J. Immunol. *42*, 374–384.

Fine, P.E.M., Carneiro, I.A.M., Milstein, J.B., and Clements, C.J. (1999). Issues relating to the use of BCG in immunization programmes. A discussion document. Department of Vaccines and Biologicals. (WHO), pp. WHO/V&B/99.23.

Fletcher, H.A., Snowden, M.A., Landry, B., Rida, W., Satti, I., Harris, S.A., Matsumiya, M., Tanner, R., O'Shea, M.K., Dheenadhayalan, V., et al. (2016). T-cell activation is an immune correlate of risk in BCG vaccinated infants. Nat. Commun. *7*, 11290.

Fremond, C.M., Togbe, D., Doz, E., Rose, S., Vasseur, V., Maillet, I., Jacobs, M., Ryffel, B., and Quesniaux, V.F. (2007). IL-1 receptor-mediated signal is an

essential component of MyD88-dependent innate response to *Mycobacterium tuberculosis* infection. J. Immunol. *179*, 1178–1189.

Frigui, W., Bottai, D., Majlessi, L., Monot, M., Josselin, E., Brodin, P., Garnier, T., Gicquel, B., Martin, C., Leclerc, C., et al. (2008). Control of *M. tuberculosis* ESAT-6 secretion and specific T cell recognition by PhoP. PLoS Pathog. *4*, e33.

Gengenbacher, M., Nieuwenhuizen, N., Vogelzang, A., Liu, H., Kaiser, P., Schuerer, S., Lazar, D., Wagner, I., Mollenkopf, H.J., and Kaufmann, S.H. (2016). Deletion of *nuoG* from the vaccine candidate *Mycobacterium bovis* BCG DeltaureC:hly improves protection against tuberculosis. MBio *7*, e00679–e16.

Grode, L., Ganoza, C.A., Brohm, C., Weiner, J., 3rd, Eisele, B., and Kaufmann, S.H. (2013). Safety and immunogenicity of the recombinant BCG vaccine VPM1002 in a phase 1 open-label randomized clinical trial. Vaccine *31*, 1340–1348.

Gröschel, M.I., Sayes, F., Simeone, R., Majlessi, L., and Brosch, R. (2016). ESX secretion systems: Mycobacterial evolution to counter host immunity. Nat. Rev. Microbiol. *14*, 677–691.

Guarda, G., Braun, M., Staehli, F., Tardivel, A., Mattmann, C., Förster, I., Farlik, M., Decker, T., Du Pasquier, R.A., Romero, P., and Tschopp, J. (2011). Type I interferon inhibits interleukin-1 production and inflammasome activation. Immunity *34*, 213–223.

Hagedorn, M., Rohde, K.H., Russell, D.G., and Soldati, T. (2009). Infection by tubercular mycobacteria is spread by nonlytic ejection from their amoeba hosts. Science *323*, 1729–1733.

Hart, P.D., and Sutherland, I. (1977). BCG and vole bacillus vaccines in the prevention of tuberculosis in adolescence and early adult life. BMJ *2*, 293–295.

Hornung, V., Ablasser, A., Charrel-Dennis, M., Bauernfeind, F., Horvath, G., Caffrey, D.R., Latz, E., and Fitzgerald, K.A. (2009). AIM2 recognizes cytosolic dsDNA and forms a caspase-1-activating inflammasome with ASC. Nature *458*, 514–518.

Hsu, T., Hingley-Wilson, S.M., Chen, B., Chen, M., Dai, A.Z., Morin, P.M., Marks, C.B., Padiyar, J., Goulding, C., Gingery, M., et al. (2003). The primary mechanism of attenuation of bacillus Calmette-Guerin is a loss of secreted lytic function required for invasion of lung interstitial tissue. Proc. Natl. Acad. Sci. USA *100*, 12420–12425.

Kamath, A.B., Woodworth, J., Xiong, X., Taylor, C., Weng, Y., and Behar, S.M. (2004). Cytolytic CD8+ T cells recognizing CFP10 are recruited to the lung after *Mycobacterium tuberculosis* infection. J. Exp. Med. *200*, 1479–1489.

Kaufmann, S.H., Evans, T.G., and Hanekom, W.A. (2015). Tuberculosis vaccines: Time for a global strategy. Sci. Transl. Med. *7*, 276fs8.

Knight, G.M., Griffiths, U.K., Sumner, T., Laurence, Y.V., Gheorghe, A., Vassall, A., Glaziou, P., and White, R.G. (2014). Impact and cost-effectiveness of new tuberculosis vaccines in low- and middle-income countries. Proc. Natl. Acad. Sci. USA *111*, 15520–15525.

Kupz, A., Zedler, U., Stäber, M., Perdomo, C., Dorhoi, A., Brosch, R., and Kaufmann, S.H. (2016). ESAT-6-dependent cytosolic pattern recognition drives noncognate tuberculosis control in vivo. J. Clin. Invest. *126*, 2109–2122.

Le Bon, A., Etchart, N., Rossmann, C., Ashton, M., Hou, S., Gewert, D., Borrow, P., and Tough, D.F. (2003). Cross-priming of CD8+ T cells stimulated by virus-induced type I interferon. Nat. Immunol. *4*, 1009–1015.

Lou, Y., Rybniker, J., Sala, C., and Cole, S.T. (2017). EspC forms a filamentous structure in the cell envelope of *Mycobacterium tuberculosis* and impacts ESX-1 secretion. Mol. Microbiol. *103*, 26–38.

MacGurn, J.A., Raghavan, S., Stanley, S.A., and Cox, J.S. (2005). A non-RD1 gene cluster is required for Snm secretion in *Mycobacterium tuberculosis*. Mol. Microbiol. *57*, 1653–1663.

Mahairas, G.G., Sabo, P.J., Hickey, M.J., Singh, D.C., and Stover, C.K. (1996). Molecular analysis of genetic differences between *Mycobacterium bovis* BCG and virulent *M. bovis*. J. Bacteriol. *178*, 1274–1282.

Majlessi, L., and Brosch, R. (2015). *Mycobacterium tuberculosis* meets the cytosol: The role of cGAS in anti-mycobacterial immunity. Cell Host Microbe *17*, 733–735.

Majlessi, L., Rojas, M.J., Brodin, P., and Leclerc, C. (2003). CD8+-T-cell responses of *Mycobacterium*-infected mice to a newly identified major histocompatibility complex class I-restricted epitope shared by proteins of the ESAT-6 family. Infect. Immun. *71*, 7173–7177.

Majlessi, L., Prados-Rosales, R., Casadevall, A., and Brosch, R. (2015). Release of mycobacterial antigens. Immunol. Rev. *264*, 25–45.

Manca, C., Tsenova, L., Freeman, S., Barczak, A.K., Tovey, M., Murray, P.J., Barry, C., and Kaplan, G. (2005). Hypervirulent *M. tuberculosis* W/Beijing strains upregulate type I IFNs and increase expression of negative regulators of the Jak-Stat pathway. J. Interferon Cytokine Res. *25*, 694–701.

McNab, F., Mayer-Barber, K., Sher, A., Wack, A., and O'Garra, A. (2015). Type I interferons in infectious disease. Nat. Rev. Immunol. *15*, 87–103.

Muruve, D.A., Pétrilli, V., Zaiss, A.K., White, L.R., Clark, S.A., Ross, P.J., Parks, R.J., and Tschopp, J. (2008). The inflammasome recognizes cytosolic microbial and host DNA and triggers an innate immune response. Nature *452*, 103–107.

Novikov, A., Cardone, M., Thompson, R., Shenderov, K., Kirschman, K.D., Mayer-Barber, K.D., Myers, T.G., Rabin, R.L., Trinchieri, G., Sher, A., and Feng, C.G. (2011). Mycobacterium tuberculosis triggers host type I IFN signaling to regulate IL-1β production in human macrophages. J. Immunol. *187*, 2540–2547.

Ordway, D., Henao-Tamayo, M., Harton, M., Palanisamy, G., Troudt, J., Shanley, C., Basaraba, R.J., and Orme, I.M. (2007). The hypervirulent *Mycobacterium tuberculosis* strain HN878 induces a potent TH1 response followed by rapid down-regulation. J. Immunol. *179*, 522–531.

Orme, I.M., Robinson, R.T., and Cooper, A.M. (2015). The balance between protective and pathogenic immune responses in the TB-infected lung. Nat. Immunol. *16*, 57–63.

Ottenhoff, T.H., and Kaufmann, S.H. (2012). Vaccines against tuberculosis: Where are we and where do we need to go? PLoS Pathog. *8*, e1002607.

Pym, A.S., Brodin, P., Brosch, R., Huerre, M., and Cole, S.T. (2002). Loss of RD1 contributed to the attenuation of the live tuberculosis vaccines *Mycobacterium bovis* BCG and *Mycobacterium microti*. Mol. Microbiol. *46*, 709–717.

Pym, A.S., Brodin, P., Majlessi, L., Brosch, R., Demangel, C., Williams, A., Griffiths, K.E., Marchal, G., Leclerc, C., and Cole, S.T. (2003). Recombinant BCG exporting ESAT-6 confers enhanced protection against tuberculosis. Nat. Med. *9*, 533–539.

Ramakrishnan, L., Federspiel, N.A., and Falkow, S. (2000). Granuloma-specific expression of *Mycobacterium* virulence proteins from the glycine-rich PE-PGRS family. Science *288*, 1436–1439.

Romagnoli, A., Etna, M.P., Giacomini, E., Pardini, M., Remoli, M.E., Corazzari, M., Falasca, L., Goletti, D., Gafa, V., Simeone, R., et al. (2012). ESX-1 dependent impairment of autophagic flux by *Mycobacterium tuberculosis* in human dendritic cells. Autophagy *8*, 1357–1370.

Ryan, A.A., Nambiar, J.K., Wozniak, T.M., Roediger, B., Shklovskaya, E., Britton, W.J., Fazekas de St Groth, B., and Triccas, J.A. (2009). Antigen load governs the differential priming of CD8 T cells in response to the bacille Calmette Guerin vaccine or *Mycobacterium tuberculosis* infection. J. Immunol. *182*, 7172–7177.

Sagoo, P., Garcia, Z., Breart, B., Lemaître, F., Michonneau, D., Albert, M.L., Levy, Y., and Bousso, P. (2016). In vivo imaging of inflammasome activation reveals a subcapsular macrophage burst response that mobilizes innate and adaptive immunity. Nat. Med. *22*, 64–71.

Saiga, H., Nieuwenhuizen, N., Gengenbacher, M., Koehler, A.B., Schuerer, S., Moura-Alves, P., Wagner, I., Mollenkopf, H.J., Dorhoi, A., and Kaufmann, S.H. (2015). The recombinant BCG DeltaureC:hly vaccine targets the AIM2 inflammasome to induce autophagy and inflammation. J. Infect. Dis. *211*, 1831–1841.

Sayes, F., Sun, L., Di Luca, M., Simeone, R., Degaiffier, N., Fiette, L., Esin, S., Brosch, R., Bottai, D., Leclerc, C., and Majlessi, L. (2012). Strong immunogenicity and cross-reactivity of *Mycobacterium tuberculosis* ESX-5 type VII

secretion: Encoded PE-PPE proteins predicts vaccine potential. Cell Host Microbe *11*, 352–363.

Sayes, F., Pawlik, A., Frigui, W., Gröschel, M.I., Crommelynck, S., Fayolle, C., Cia, F., Bancroft, G.J., Bottai, D., Leclerc, C., et al. (2016). CD4+ T cells recognizing PE/PPE antigens directly or via cross reactivity are protective against pulmonary *Mycobacterium tuberculosis* infection. PLoS Pathog. *12*, e1005770.

Simeone, R., Bobard, A., Lippmann, J., Bitter, W., Majlessi, L., Brosch, R., and Enninga, J. (2012). Phagosomal rupture by *Mycobacterium tuberculosis* results in toxicity and host cell death. PLoS Pathog. *8*, e1002507.

Simeone, R., Sayes, F., Song, O., Gröschel, M.I., Brodin, P., Brosch, R., and Majlessi, L. (2015). Cytosolic access of *Mycobacterium tuberculosis*: Critical impact of phagosomal acidification control and demonstration of occurrence in vivo. PLoS Pathog. *11*, e1004650.

Simeone, R., Majlessi, L., Enninga, J., and Brosch, R. (2016). Perspectives on mycobacterial vacuole-to-cytosol translocation: The importance of cytosolic access. Cell. Microbiol. *18*, 1070–1077.

Spertini, F., Audran, R., Chakour, R., Karoui, O., Steiner-Monard, V., Thierry, A.C., Mayor, C.E., Rettby, N., Jaton, K., Vallotton, L., et al. (2015). Safety of human immunisation with a live-attenuated *Mycobacterium tuberculosis* vaccine: A randomised, double-blind, controlled phase I trial. Lancet Respir. Med. *3*, 953–962.

Stamm, L.M., Morisaki, J.H., Gao, L.Y., Jeng, R.L., McDonald, K.L., Roth, R., Takeshita, S., Heuser, J., Welch, M.D., and Brown, E.J. (2003). *Mycobacterium marinum* escapes from phagosomes and is propelled by actin-based motility. J. Exp. Med. *198*, 1361–1368.

Stanley, S.A., Johndrow, J.E., Manzanillo, P., and Cox, J.S. (2007). The Type I IFN response to infection with *Mycobacterium tuberculosis* requires ESX-1-mediated secretion and contributes to pathogenesis. J. Immunol. *178*, 3143–3152.

Stinear, T.P., Seemann, T., Harrison, P.F., Jenkin, G.A., Davies, J.K., Johnson, P.D., Abdellah, Z., Arrowsmith, C., Chillingworth, T., Churcher, C., et al. (2008). Insights from the complete genome sequence of *Mycobacterium marinum* on the evolution of *Mycobacterium tuberculosis*. Genome Res. *18*, 729–741.

Sula, L., and Radkovský, I. (1976). Protective effects of *M. microti* vaccine against tuberculosis. J. Hyg. Epidemiol. Microbiol. Immunol. *20*, 1–6.

Uplekar, M., Weil, D., Lonnroth, K., Jaramillo, E., Lienhardt, C., Dias, H.M., Falzon, D., Floyd, K., Gargioni, G., Getahun, H., et al.; WHO's Global TB Programme (2015). WHO's new end TB strategy. Lancet *385*, 1799–1801.

van der Wel, N., Hava, D., Houben, D., Fluitsma, D., van Zon, M., Pierson, J., Brenner, M., and Peters, P.J. (2007). *M. tuberculosis* and *M. leprae* translocate from the phagolysosome to the cytosol in myeloid cells. Cell *129*, 1287–1298.

Wang, J., McIntosh, F., Radomski, N., Dewar, K., Simeone, R., Enninga, J., Brosch, R., Rocha, E.P., Veyrier, F.J., and Behr, M.A. (2015). Insights on the emergence of *Mycobacterium tuberculosis* from the analysis of *Mycobacterium kansasii*. Genome Biol. Evol. *7*, 856–870.

Wassermann, R., Gulen, M.F., Sala, C., Perin, S.G., Lou, Y., Rybniker, J., Schmid-Burgk, J.L., Schmidt, T., Hornung, V., Cole, S.T., and Ablasser, A. (2015). *Mycobacterium tuberculosis* differentially activates cGAS- and inflammasome-dependent intracellular immune responses through ESX-1. Cell Host Microbe *17*, 799–810.

Watson, R.O., Manzanillo, P.S., and Cox, J.S. (2012). Extracellular *M. tuberculosis* DNA targets bacteria for autophagy by activating the host DNA-sensing pathway. Cell *150*, 803–815.

Watson, R.O., Bell, S.L., MacDuff, D.A., Kimmey, J.M., Diner, E.J., Olivas, J., Vance, R.E., Stallings, C.L., Virgin, H.W., and Cox, J.S. (2015). The Cytosolic Sensor cGAS Detects *Mycobacterium tuberculosis* DNA to Induce Type I Interferons and Activate Autophagy. Cell Host Microbe *17*, 811–819.

Wiens, K.E., and Ernst, J.D. (2016). The mechanism for Type I interferon induction by *Mycobacterium tuberculosis* is bacterial strain-dependent. PLoS Pathog. *12*, e1005809.

Wong, K.W., and Jacobs, W.R., Jr. (2011). Critical role for NLRP3 in necrotic death triggered by *Mycobacterium tuberculosis*. Cell. Microbiol. *13*, 1371–1384.

Woodworth, J.S., Fortune, S.M., and Behar, S.M. (2008). Bacterial protein secretion is required for priming of CD8+ T cells specific for the *Mycobacterium tuberculosis* antigen CFP10. Infect. Immun. *76*, 4199–4205.

Zhang, L., Ru, H.W., Chen, F.Z., Jin, C.Y., Sun, R.F., Fan, X.Y., Guo, M., Mai, J.T., Xu, W.X., Lin, Q.X., and Liu, J. (2016). Variable virulence and efficacy of BCG vaccine strains in mice and correlation with genome polymorphisms. Mol. Ther. *24*, 398–405.

Cell Reports, Volume *18*

Supplemental Information

Recombinant BCG Expressing ESX-1 of *Mycobacterium marinum* Combines Low Virulence with Cytosolic Immune Signaling and Improved TB Protection

Matthias I. Gröschel, Fadel Sayes, Sung Jae Shin, Wafa Frigui, Alexandre Pawlik, Mickael Orgeur, Robin Canetti, Nadine Honoré, Roxane Simeone, Tjip S. van der Werf, Wilbert Bitter, Sang-Nae Cho, Laleh Majlessi, and Roland Brosch

***M. marinum* M**

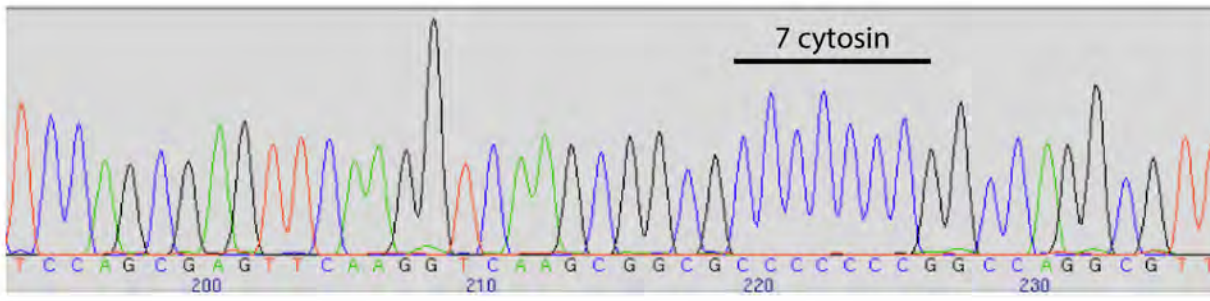

pRD1-*Mmar* (non-repaired vector insert)

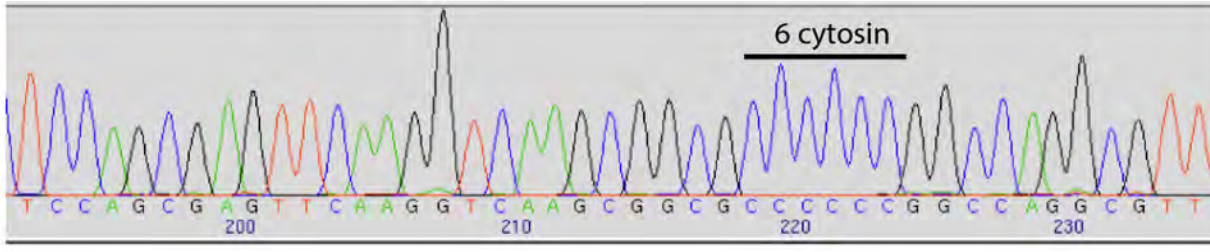

***M. marinum* M^{Pasteur}**

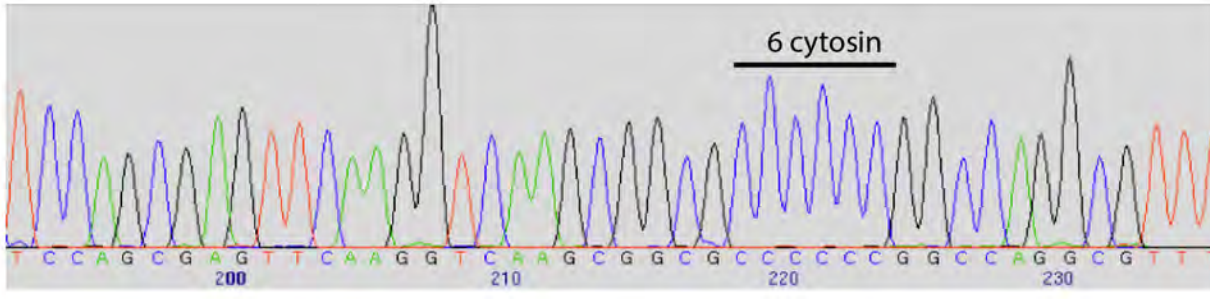

***M. marinum* M^{VU}**

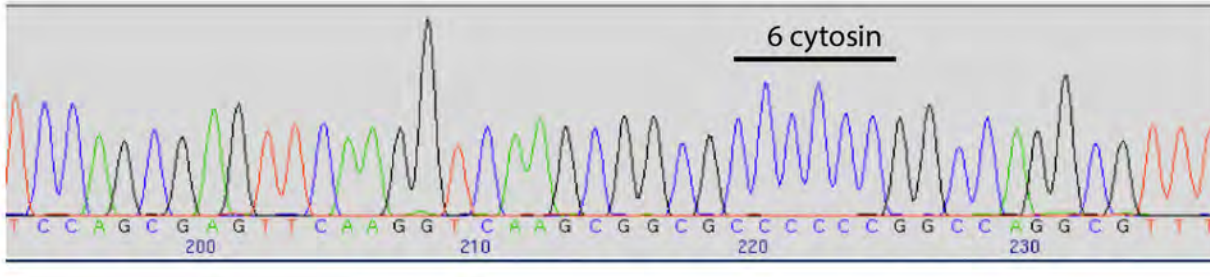

Figure S1, Related to Figure 1. Sequence polymorphisms in the coding region of the *eccCb*$_1$ gene of different *M. marinum* M variants and the original pRD1-*Mmar* cosmid sequence.

A

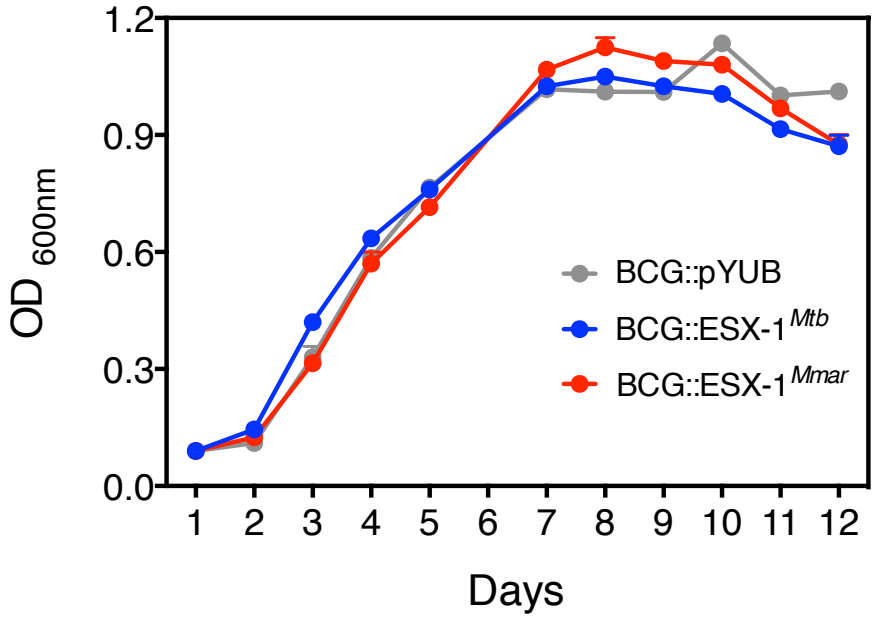

B

ESAT-6 *M. tuberculosis vs* ESAT-6 *M. marinum*

Amino Acid Alignment statistics

Score	Expect	Method	Identities	Positives	Gaps
175 bits(443)	4e-64	Compositional matrix adjust.	87/95(92%)	92/95(96%)	0/95(0%)

```
Query  1   MTEQQWNFAGIEAAASAIQGNVTSIHSLLDEGKQSLTKLAAAWGGSGSEAYQGVQQKWDA  60
           MTEQQWNFAGIEAA+SAIQGNVTSIHSLLDEGKQSL KLAAAWGGSGSEAY+GVQQ WD+
Sbjct  1   MTEQQWNFAGIEAASSAIQGNVTSIHSLLDEGKQSLHKLAAAWGGSGSEAYRGVQQNWDS 60

Query  61  TATELNNALQNLARTISEAGQAMASTEGNVTGMFA 95
           TA ELNN+LQNLARTISEAGQAM+STEGNVTGMFA
Sbjct  61  TAQELNNSLQNLARTISEAGQAMSSTEGNVTGMFA 95
```

CFP-10 *M. tuberculosis vs* CFP-10 *M. marinum*

Amino Acid Alignment statistics

Score	Expect	Method	Identities	Positives	Gaps
191 bits(485)	3e-70	Compositional matrix adjust.	97/100(97%)	98/100(98%)	0/100(0%)

```
Query  1   MAEMKTDAATLAQEAGNFERISGDLKTQIDQVESTAGSLQGQWRGAAGTAAQAAVVRFQE  60
           MAEMKTDAATLAQEAGNFERISGDLKTQIDQVESTAGSLQ QWRGAAGTAAQAAVVRFQE
Sbjct  1   MAEMKTDAATLAQEAGNFERISGDLKTQIDQVESTAGSLQAQWRGAAGTAAQAAVVRFQE  60

Query  61  AANKQKQELDEISTNIRQAGVQYSRADEEQQQALSSQMGF  100
           AANKQK ELDEISTNIRQAGVQYSRAD+EQQQALSSQMGF
Sbjct  61  AANKQKAELDEISTNIRQAGVQYSRADDEQQQALSSQMGF  100
```

Figure S2, Related to Figure 1. A. Comparative growth curve of different recombinant BCG strains in Dubos liquid medium at 37°C. **B.** Protein sequence identities between *M. tuberculosis* and *M. marinum* ESAT-6 or CFP-10, as determined by BLAST.

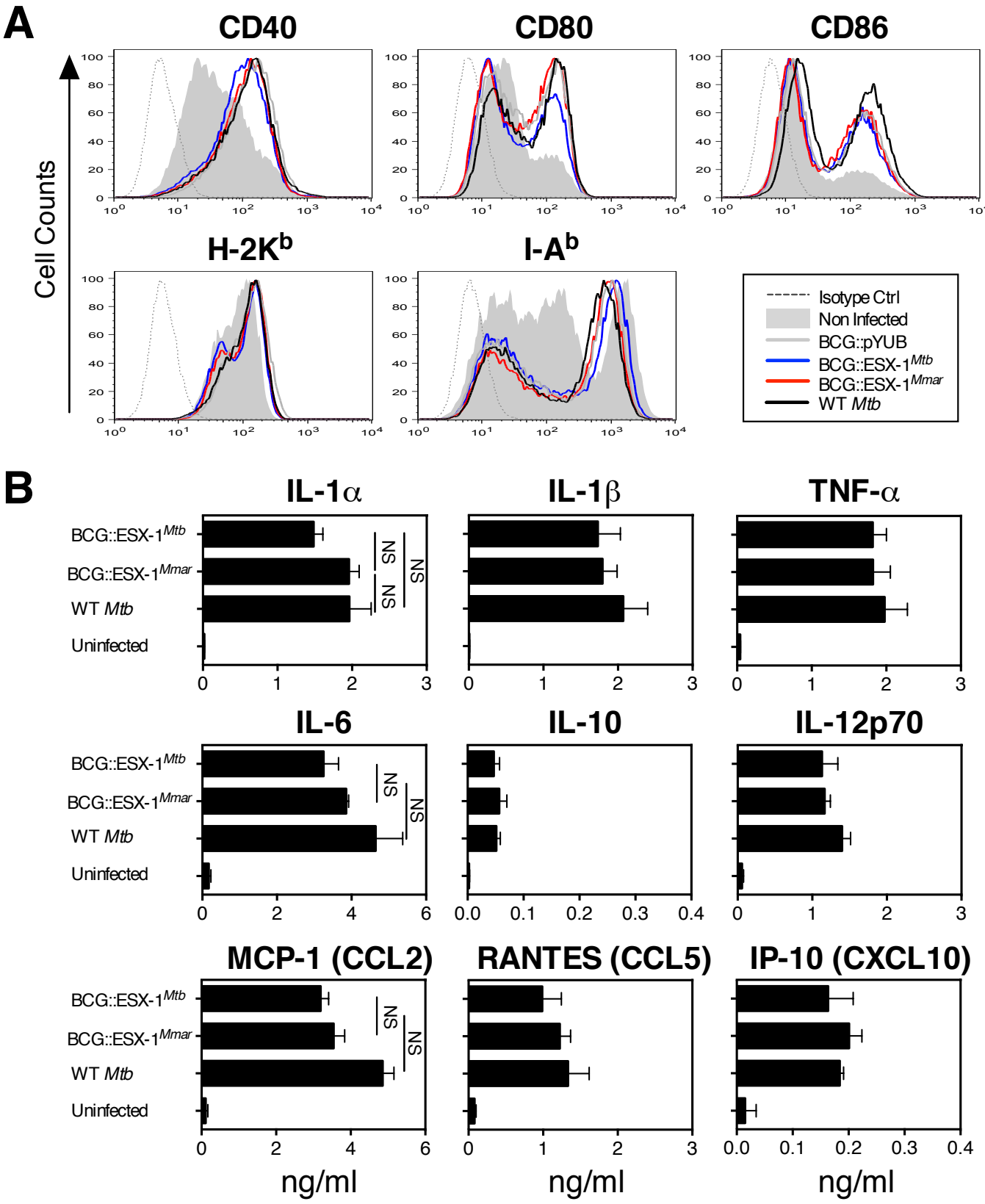

Figure S3. Phenotypic and functional activation of innate immune cells induced by BCG::ESX-1^{Mmar}, Related to Figure 3. A. Phenotypic maturation of BM-DCs from C57BL/6 mice infected *in vitro* by different BCG strains (M.O.I. = 1), as judged by cytometric evaluation of surface expression of co-stimulatory or MHC-I or -II molecules at 12h post infection. **B.** Functional maturation of the same infected BM-DCs, as determined by pro- or anti-inflammatory cytokine and chemokine quantifications in the supernatants of culture by Multiplexassay. Error bars represent SD. NS = not significant, as determined by One Way ANOVA test with Tukey's correction. The results are representative at least of two independent experiments.

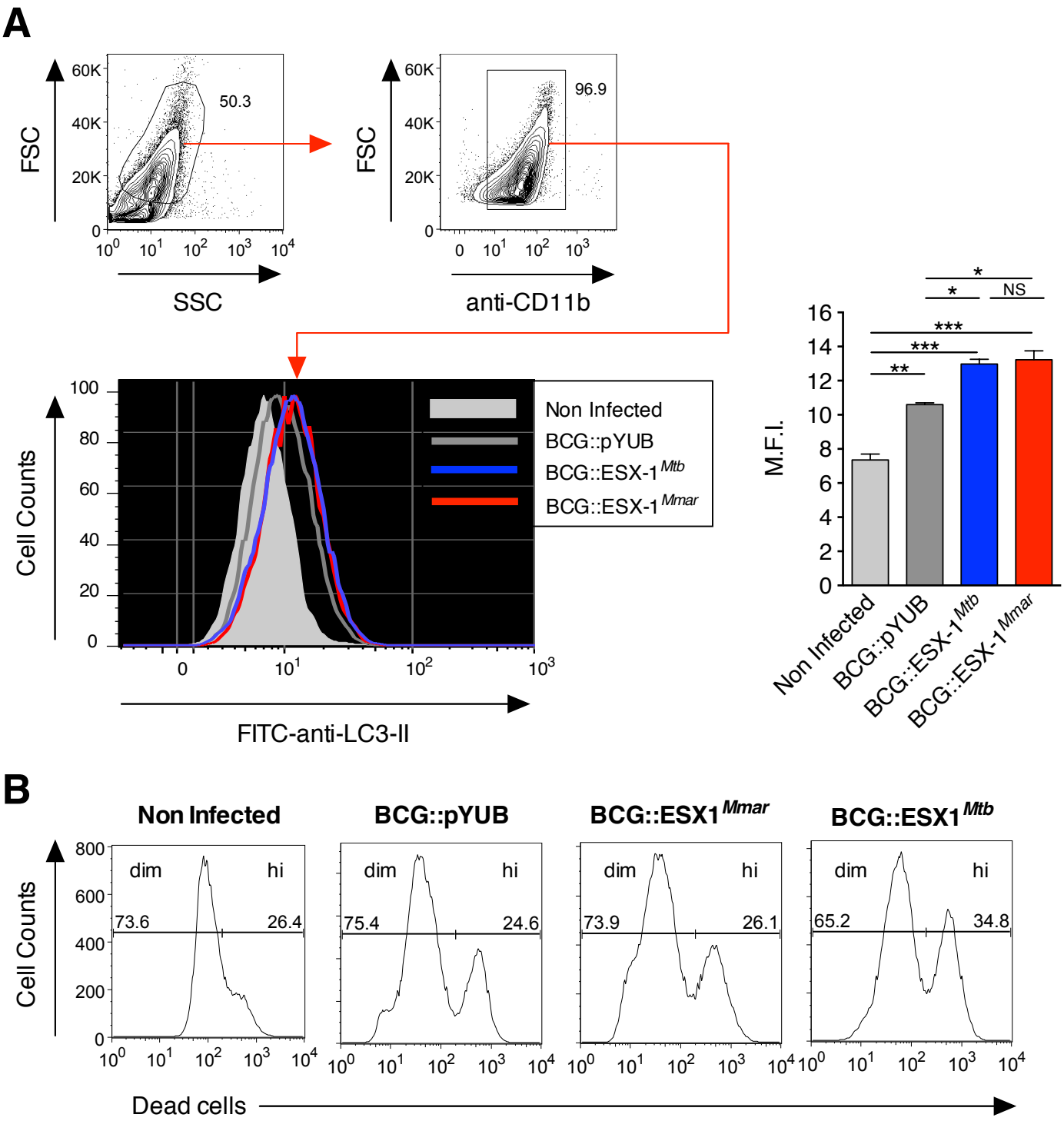

Figure S4, Related to Figure 3. A. Gating strategy and intensities of intracellular LC3-II expression in THP-1 cells infected with different BCG strains (M.O.I. = 10) at 6h post infection, as evaluated by flow cytometry. NS = not significant, *, ** or *** = statistically significant, as determined by One Way ANOVA test with Tukey's correction, with $p < 0.05$, $p < 0.005$ or $p < 0.001$, respectively. **B.** Parallel evaluation of the viability of THP-1 cells, in the same culture wells. Proportions of live (dim) and dead (hi) cells within the CD11b$^+$ population are evaluated by Live/Dead (Invitrogen) staining. The results are representative of two independent experiments.

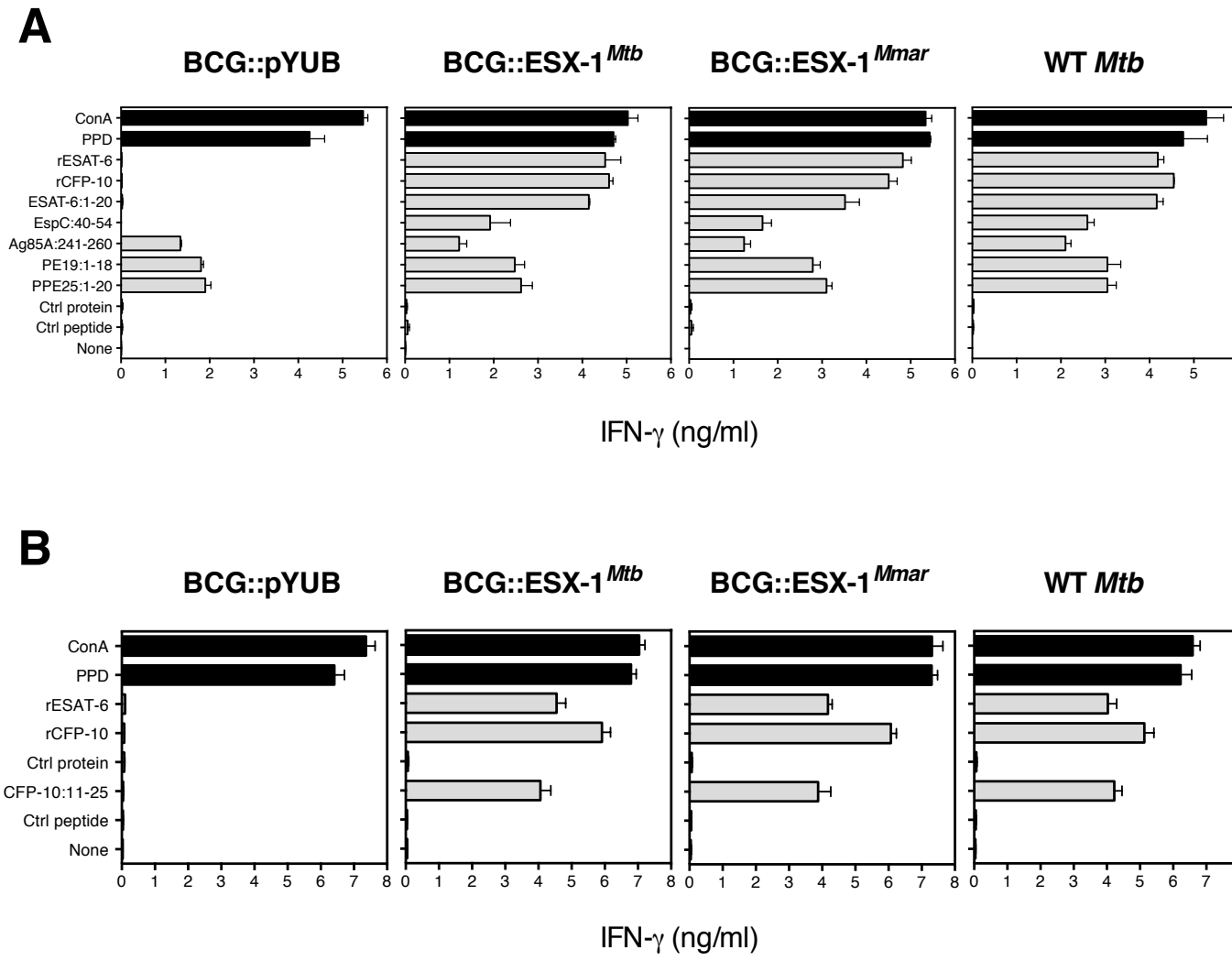

Figure S5. T-cell immunogenicity of BCG::ESX-1 *Mmar* in immunocompetent C57BL/6 (H-2^b) and C3H (H-2^k) mice, Related to Figure 4. T-cell IFN-γ responses of C57BL/6 (**A**) or C3H mice (**B**) (*n* = 3 per group) immunized s.c. with 1 x 10^6 CFU/mouse of different mycobacterial strains, as assessed at 4 wks post-immunization. Total splenocytes of the immunized mice were stimulated *in vitro* with different mycobacterial antigens during 72h. Concanavalin A and Purified Protein Derivative (PPD) were used as positive control while rMalE protein and MalE:100-114 peptide were used as negative controls. Error bars represent SD. The results are representative at least of two independent experiments.

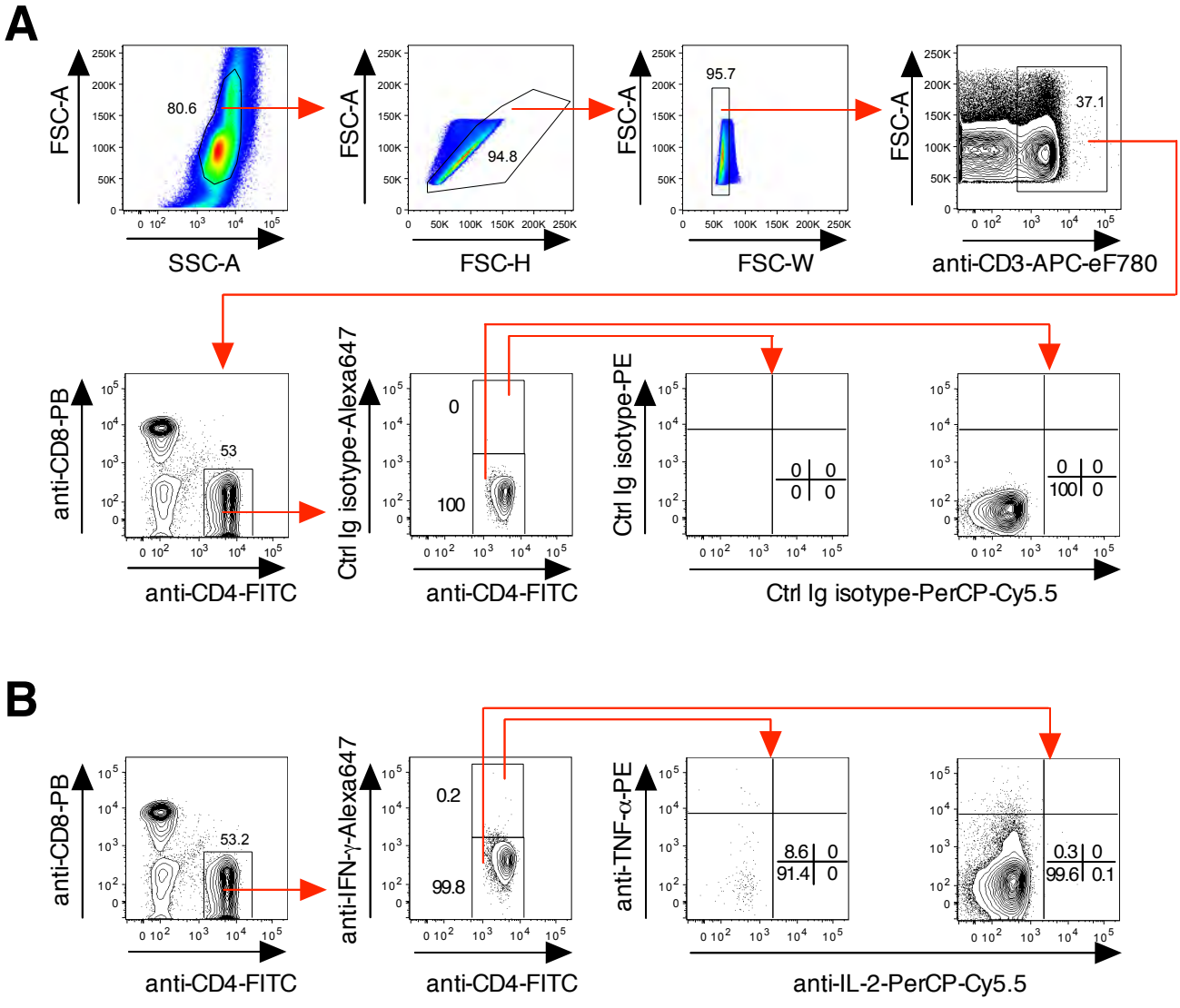

Figure S6. Negative controls for ICS assay performed to dissect Th1 subsets in the spleen of BCG::ESX-1^{Mmar}-immunized mice, Related to Figure 4. A-B. Gating strategy and cytometric analyses to identify different subsets of Th1 effectors in the splenocytes of BCG::ESX-1^{Mmar}-immunized C57BL/6 mice stimulated *in vitro* with 10 μg/ml of PPE25:1-20 peptide and stained with control Ig isotypes (**A**) or stimulated with 10 μg/ml of the MalE: 100-114 negative control peptide and stained with cytokine-specific mAbs (**B**). Cytometric plots represent 5% contours with outliers, representative of 3 mice per group.

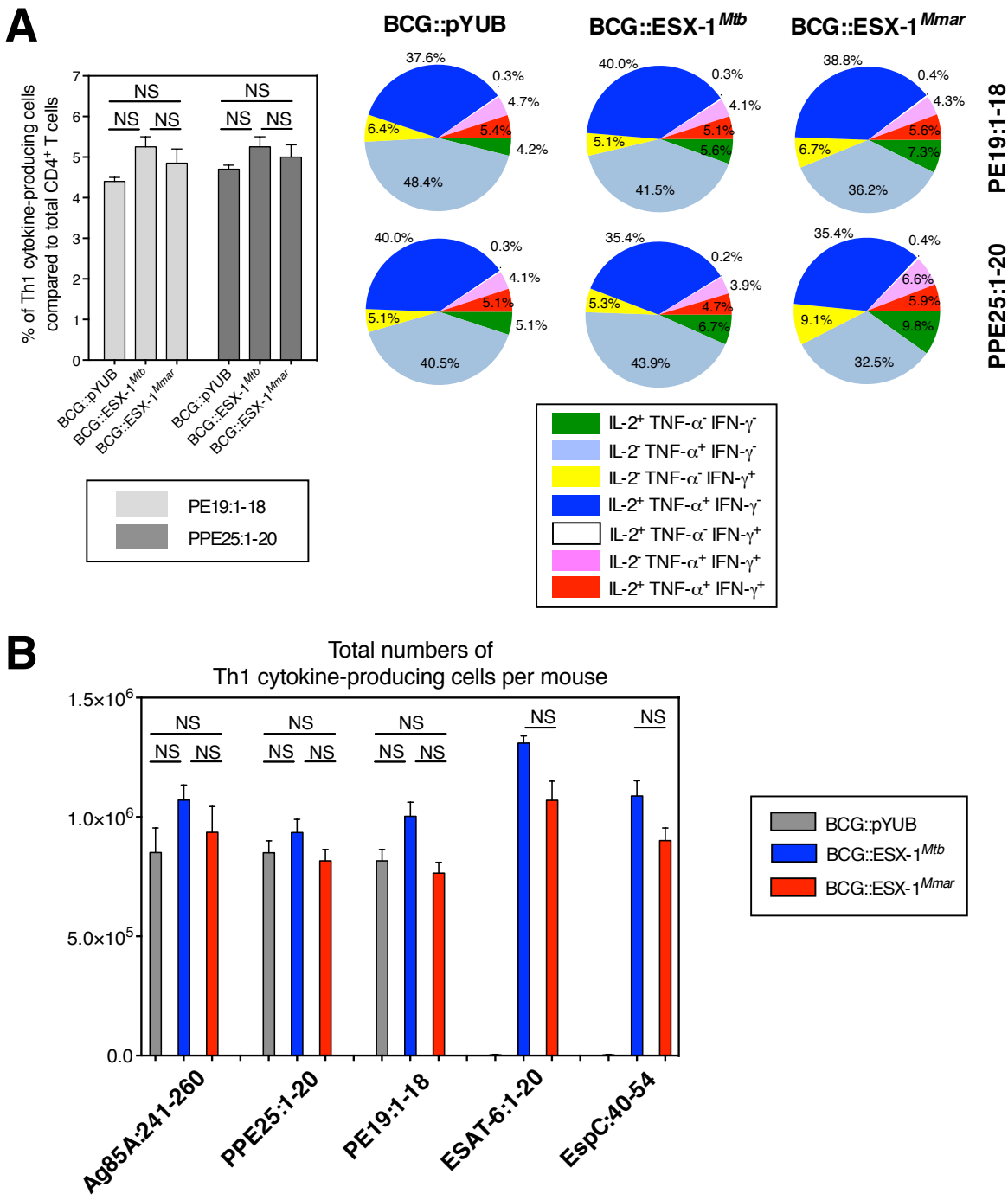

Figure S7. Th1-cell responses against PE/PPE proteins induced by BCG::ESX-1^{Mmar} immunization, Related to Figure 4. A. Profile of Th1 cytokine-producing CD4$^+$ T cells, specific to ESX-5-associated PE19 or PPE25 mycobacterial antigens, in the spleen of C57BL/6 mice (n = 3 per group) at 28 days post immunization with 1 x 10^6 CFU/mouse of different BCG strains. Total splenocytes from each group were stimulated *in vitro* with 10 μg/ml of PE19:1-18 or PPE25:1-20 synthetic peptide containing I-A^b-restricted immunodominant epitopes, prior to ICS in order to determine frequencies of single, double or triple IL-2, TNF-α and IFN-γ cytokine-producing CD4$^+$ T cells. **B.** Absolute numbers of total Th1 cytokine-producing effector cells in the spleen of the same immunized mice described in Fig 4 and Fig S6. These absolute numbers of Th1 effectors specific to individual antigen were calculated for each group based on their percentage obtained from ICS by flow cytometric analyses. Error bars represent SD. NS = not significant, as determined by One Way ANOVA test with Tukey's correction.

Supplemental Experimental Procedures (Document S1)

Mycobacterial strains

Mycobacterial strains (*M. tuberculosis* H37Rv, BCG Pasteur 1173P2 and Danish 1331) held as stocks at the Institut Pasteur were grown in Dubos broth medium complemented with Albumine, Dextrose and Catalse (ADC, Difco, Becton Dickinson, Le Pont-de-Claix, France). The mycobacterial concentrations were determined by OD_{600nm} measurement and CFU counting on Middlebrook 7H11 solid Agar medium complemented with Oleic acid, Albumine, Dextrose and Catalse (OADC, Difco, Becton Dickinson) after 16-18 days of incubation at 37°C.

The two challenge *M. tuberculosis* strains HN878 and M2 were obtained from the strain collections of the International Tuberculosis Research Center (ITRC, Changwon, Gyeongsangnam-do, Korea).

Preparation and reparation of cosmid DNA

The genetic construct containing the ESX-1 region of *M. marinum* in the integrating cosmid vector pYUB412 was obtained by sub-cloning a 38.7 kb-sized *Spe*I fragment from a clone of an *M. marinum* M strain BAC library (Stinear et al., 2008) into the unique *Nhe*I site of integrating cosmid vector pYUB412 (Bange et al., 1999). Repair of a frameshift mutation in the cosmid was undertaken using a phage lambda Red-based approach, as described (Chaveroche et al., 2000). Selection of the repaired clone was facilitated by the temporary introduction of an apramycin cassette into the *esx-1* locus next to the repaired nucleotide, which required a synonymous codon change for creating an *Spe*I restriction site. After sequence verification, cosmid DNA was freshly prepared from a strain of recombinant *Escherichia coli* DH10B (Invitrogen Corporation, Cergy Pontoise, France) that contained the repaired cosmid. *M. bovis* BCG Pasteur 1173P2, held at Institut Pasteur, was grown at 37°C on Middlebrook 7H11 medium (Difco) supplemented with OADC. To obtain electrocompetent cells, bacteria from solid culture were transferred into 7H9 medium complemented with ADC and grown for 10 days. Cells were harvested and washed twice with H_2O and once with 10% Glycerol at RT. The pellet was resuspended in 2 ml of 10% glycerol. The cell suspension was mixed with the integrative ESX-1 cosmids and electroporated using a Bio-Rad gene pulser XCell (Marnes-la-Coquette, France) at 2.5 kV. Electroporated cells were cultured overnight at 37°C and then plated on 7H11 medium containing hygromycin 50

µg/ml. Antibiotic resistant colonies were collected after ≈ 3 weeks and analyzed for the presence of the integrated cosmid.

Antigen presenting assay

Several MHC-II-restricted T-cell hybridomas specific to mycobacterial antigens were used in order to detect the secretion by mycobacteria, which leads to the antigenic presentation by the infected BM-DC of different ESX-1 substrates, as follows: I-A^b-restricted NB11 (specific to ESAT-6:1-20) (Frigui et al., 2008; Majlessi et al., 2006). IF1 (specific to EspC:40-54) and I-A^k-restricted XE12 (specific to CFP-10:11-25) (Sayes et al., 2016, manuscript in preparation). DE10 T-cell hybridoma (specific to Ag85A:241-260) (Majlessi et al., 2006) were used as an ESX-1-independent control antigen. BM-DCs were obtained from femurs of 8-10-week-old female C57BL/6JRj (H-2^b) or C3H/HeJ (H-2^k) mice (Janvier, Le Genest-Saint-Isle, France), depending on the MHC restriction of the T-cell epitopes to be studied and as described previously (Sayes et al., 2012). BM-DCs plated at 2 x 10^5 cells/well in flat-bottom, 96-well culture plates in completed, antibiotic-free RPMI 1640. Four hours later, BM-DCs were infected with various M.O.I of mycobacteria. After over-night incubation, the infected DCs were washed twice prior to the addition of 1 x 10^5 cells per well of the T-cell hybridomas of interest in 100 µl. After over-night incubation, specific IL-2 produced by T-cell hybridomas was quantified in the co-culture supernatants using ELISA.

ELISA & Multiplex cytokine/chemokine assays

Levels of IL-1α, IL-1β, TNF-α, IL-6, IL-10, IL-12p70, MCP-1 (CCL2), RANTES (CCL5), IP-10 (CXCL10) in the BM-DC culture supernatants were determined by multiple ProcartaPlex (Affymetrix) kit assays according to the manufacturer's protocol and a Luminex X-100 Reader. For ELISA experiments, monoclonal antibodies (mAbs) specific to murine IL-2 or IFN-γ were purchased from BD Pharmingen (Le pont-de-Claix, France). Murine TNF-α-specific mAbs were obtained from eBioscience (Paris, France). Human IL-1β and IFN-β were quantified using the DY201-05 (R&D Systems) and 41410 (PBL Assay Science) kits, respectively.

FRET assay by flow cytometry

The principle of the β-lactamase CCF-4 assay has recently been described (Simeone et al., 2015). In short, human pro-monocytic THP-1 cells were plated in 24-well plate at 5 x 10^5 cells/well in 2 ml of RPMI complemented with 10% FCS, in the presence of 20 ng/ml of

PMA (Phorbol 12-myristate 13-acetate, Sigma Aldrich) for 72h. Upon 2h incubation with different mycobacterial strains at an multiplicity of infection (M.O.I.) of 0.5, cells were washed three times with PBS. Fresh medium was added and cells were incubated for 4 days. After staining with anti-CD11b-APC (BD Pharmingen) and CCF-4 (Invitrogen), cells were analyzed on a CyAn cytometer system (Beckman Coulter, Villepinte, France). Phagosomal rupture was observed once the CCF-4 signal switched from green (535 nm) to blue (447nm), when CCF-4 was not cleaved the signal remained green.

Intracellular detection of LC3-II

PMA-differentiated THP-1 cells plated in 12-well plates at 1 x 10^6 per well were infected at an M.O.I. of 10 with the different mycobacterial strains. At 6h post-infection, cells were washed and stained with APC-anti-CD11b mAb. Next, permeabilization and intracellular staining with FITC-anti-LC3-II mAb was performed by use of a Millipore (Temecula, CA, USA) autophagy detection reagent pack according to the manufacturer's instructions.

Immunogenicity and T-cell assay

For immunological studies 6-8-week-old female C3H and C57BL/6 mice (Janvier) were immunized s.c. with 1 x 10^6 CFU of the mycobacterial strains in 200 µl PBS, as previously described (Sayes et al., 2012). After 3-4 weeks, splenocytes from each group were cultured on 96 well plates (1 x 10^6 cells/well) using 2mM GlutaMax complemented HL-1 medium (Biowhittaker, Lonza, France) in the presence of various mycobacterial antigens. After 72h of incubation IFN-γ was quantified in culture supernatants using ELISA.

T-cell intracellular Th1 cytokine assay

Splenocytes of immunized C57BL/6 mice (n = 2-3 mice per group) were cultured in 24 wells plate at 1 x 10^7 cells/well. Cells were stimulated with 10 µg/ml of different peptides in the presence of 1 µg/ml anti-CD28 (clone 37.51) and 1 µg/ml of anti-CD49d (clone 9C10-MFR4.B) mAbs (BD Pharmingen) during 12-14h at 37°C 5% CO_2. Upon 3h of incubation with Golgi Plug (Brefeldin A, BD Pharmingen), cells were harvested and stained with appropriate dilutions of AlloPhycoCyanin (APC)-eFluor780-anti-CD3ε, FITC-anti-CD4 and/or PB-anti-CD8α mAbs (BD Pharmingen) at 4°C in dark. To perform the ICS assay the surface stained cells were permeabilized using Cytofix/Cytoperm (BD Pharmingen) and incubated with appropriate dilutions of PerCP-Cyanine5.5-anti-IL-2 (clone JES6-5H4,

eBioscience), PE-anti-TNF-α (clone 554419, BD Pharmingen) and Alexa Fluor647-anti-IFN-γ (clone XMG1.2, eBioscience) mAbs or appropriate Ig isotypes during 30 minutes at 4°C. Finally, cells were washed twice in PermWash buffer followed by FACS buffer (PBS containing 3% Fetal Bovin Serum and 0.1% NaN_3) and then fixed with 4% PFA overnight at 4°C. The stained cells (1 x 10^6/sample) were acquired in an LSR Fortessa flow cytometer system by use of BD FACS Diva software (BD Bioscience).

In vivo experiments

Studies in immunocompetent and immunodeficient mice were performed according to European and French guidelines (Directive 86/609/CEE and Decree 87– 848 of 19 October 1987) after approval by the Institut Pasteur Safety, Animal Care and Use Committee (Protocol 11.245) and local ethical committees (CETEA 2012– 0005 and CETEA 2013– 0036). For virulence studies six-week-old female SCID mice (Janvier) were infected intravenously with 200 µl of 5 × 10^6 bacteria/mouse, and the survival of mice was monitored. The humane endpoint was defined as loss of >20% of bodyweight. Sample size choice was determined by taking into account the rule of 3Rs (replacement, reduction, refinement) and statistical requirements.

For protection experiments using *M. tuberculosis* H37Rv as challenge, six week-old female C57BL/6 mice were left unvaccinated or were immunized s.c. with 1 x 10^6 CFU/mouse with the different BCG strains. One month later, mice were challenged with ≈ 150 CFU of virulent *M. tuberculosis* H37Rv WT strain per mouse by use of a homemade nebulizer via aerosol route of infection as described (Sayes et al., 2012). CFU counts in the lungs of the challenged mice were determined at day one. Four weeks post infection, mice were sacrificed and CFU in lungs and spleen were determined.

For protection experiments using challenges with clinical *M. tuberculosis* strains HN878 or M2, specific pathogen-free female C57BL/6N at 6 weeks of age were purchased from Japan SLC, Inc. (Shijuoka, Japan) and were maintained under barrier conditions in a BL-3 biohazard animal facility at the Yonsei University Medical Research Center in an environment with a constant temperature (24±1°C) and humidity (50±5%). The animals were fed a sterile commercial mouse diet and were provided with water ad libitum under standardized light-controlled conditions (12-h light and dark periods). The mice were monitored daily, and none of the mice exhibited any clinical symptoms or illness during the experimental period.

BCG-vaccinated groups were subcutaneously immunized one time with 2.0×10^5 CFU of each BCG strain (Figure 9A). To study the protective efficacy of the vaccine strains, mice were challenged at 10 weeks post immunization with strains HN878 or M2. Briefly, the mice were exposed to a predetermined dose of the *M. tuberculosis* HN878 or M2 strain for 60 min in the inhalation chamber of an airborne infection apparatus (Glas-Col, Terre Haute, IN, USA) to expose the mice to approximately 200 CFU of viable *M. tuberculosis*. At 16 weeks post-challenge, mice were killed and numbers of viable bacteria in the lungs and the spleens of the mice were evaluated. Briefly, the bacterial count in left-superior lobes of the lungs and spleens was determined by plating organ homogenates on Middlebrook 7H11 agar (Becton Dickinson, Franklin Lakes, NJ, USA) supplemented with 10% OADC enrichment medium until the late exponential phase. CFU counts were performed after 4 weeks of incubation at 37°C. Lung samples collected for histopathology were preserved overnight in 10% normal buffered formalin, embedded with paraffin, sliced into 4- to 5-μm-thick sections, and stained with hematoxylin-eosin (H&E). The superior lobes of the right lung were stained with H&E to assess the severity of inflammation. The level of inflammation in the lungs was evaluated using ImageJ software (National Institutes of Health, USA).

All animal studies involving *M. tuberculosis* HN878 and M2 challenges were performed in accordance with Korean Food and Drug Administration (KFDA) guidelines. The experimental protocols used in this study were reviewed and approved by the Ethics Committee and Institutional Animal Care and Use Committee (Permit Number: 2015-0274) of the Laboratory Animal Research Center at Yonsei University College of Medicine (Seoul, Korea).

Statistical Analyses

GraphPad Prism software (GraphPad Software, La Jolla, CA) was used to perform statistical analyses. The One Way ANOVA test with Tukey's correction was employed to analyze the obtained data with multiple comparisons.

The data from the *in vivo* experiments with HN878 and M2 strains are reported as the medians ± interquartile range (IQR). The significance of differences between two groups was determined using unpaired Student's *t*-tests or the significance of differences between three or more groups was evaluated with one-way ANOVA followed by Dunnett's multiple comparison test using statistical software (GraphPad Prism Software, version 5.01; San Diego, CA, USA). $*p < 0.05$, $**p < 0.01$ and $***p < 0.001$ were considered statistically significant.

References (Supplemental dataset)

Bange, F.C., Collins, F.M., and Jacobs, W.R., Jr. (1999). Survival of mice infected with *Mycobacterium smegmatis* containing large DNA fragments from *Mycobacterium tuberculosis*. Tuber Lung Dis *79*, 171-180.

Chaveroche, M.K., Ghigo, J.M., and d'Enfert, C. (2000). A rapid method for efficient gene replacement in the filamentous fungus *Aspergillus nidulans*. Nucleic Acids Res *28*, E97.

Frigui, W., Bottai, D., Majlessi, L., Monot, M., Josselin, E., Brodin, P., Garnier, T., Gicquel, B., Martin, C., Leclerc, C.*, et al.* (2008). Control of *M. tuberculosis* ESAT-6 secretion and specific T cell recognition by PhoP. PLoS Pathog *4*, e33.

Majlessi, L., Simsova, M., Jarvis, Z., Brodin, P., Rojas, M.J., Bauche, C., Nouze, C., Ladant, D., Cole, S.T., Sebo, P.*, et al.* (2006). An increase in antimycobacterial Th1-cell responses by prime-boost protocols of immunization does not enhance protection against tuberculosis. Infect Immun *74*, 2128-2137.

Sayes, F., Sun, L., Di Luca, M., Simeone, R., Degaiffier, N., Fiette, L., Esin, S., Brosch, R., Bottai, D., Leclerc, C.*, et al.* (2012). Strong immunogenicity and cross-reactivity of *Mycobacterium tuberculosis* ESX-5 Type VII Secretion- encoded PE-PPE proteins predicts vaccine potential. Cell Host Microbe *11*, 352-363.

Simeone, R., Sayes, F., Song, O., Groschel, M.I., Brodin, P., Brosch, R., and Majlessi, L. (2015). Cytosolic Access of *Mycobacterium tuberculosis*: Critical Impact of Phagosomal Acidification Control and Demonstration of Occurrence In Vivo. PLoS Pathog *11*, e1004650.

Stinear, T.P., Seemann, T., Harrison, P.F., Jenkin, G.A., Davies, J.K., Johnson, P.D., Abdellah, Z., Arrowsmith, C., Chillingworth, T., Churcher, C.*, et al.* (2008). Insights from the complete genome sequence of *Mycobacterium marinum* on the evolution of *Mycobacterium tuberculosis*. Genome Res *18*, 729-741.